

1 Type of paper: full length article (Canadian Geotechnical Journal)

2 Date text written: Mar 2024

3 Number of words = 10936

4 Number of figures = 9

5 Number of tables = 3

6
7 -----
8
9 **Effective thermal conductivity of granular soils: a review of influencing factors and**
10 **prediction models towards an investigation framework through multiscale characters**

11 Author 1

12 Tairu Chen, ME, BE

13 Department of Infrastructure Engineering, The University of Melbourne, Parkville, Australia

14 ORCID: 0000-0003-4910-1980

15 Email: tairu.chen1@unimelb.edu.au

16
17 Author 2

18 Wenbin Fei✉, PhD, ME, BE

19 ¹College of Civil Engineering, Hunan University, Changsha, Hunan 410082, PRC

20 ²Key Laboratory of Building Safety and Energy Efficiency of the Ministry of Education, Hunan
21 University, Changsha 410082, PRC

22 ³Department of Infrastructure Engineering, The University of Melbourne, Parkville, Australia

23 ORCID: 0000-0002-9275-8403

24 Email: wenbinfei@outlook.com

25
26 Author 3

27 Guillermo A. Narsilio, PhD, MSc (Math), MSc (CE), CEng

28 Department of Infrastructure Engineering, The University of Melbourne, Parkville, Australia

29 ORCID: 0000-0003-1219-5661

30 Email: narsilio@unimelb.edu.au

31
32
33
34
35
36
37
38
39
40
41
42
43
44
45 **Full contact details of corresponding author**

46 Wenbin Fei, Professor

47 A316, College of Civil Engineering, Hunan Univ., Changsha, Hunan 410082, PRC

48 Email: wenbinfei@outlook.com

50 **Abstract:**

51 The effective thermal conductivity of soil is important to geo-engineering applications, and it
52 is controlled by factors across different length scales. Through a comprehensive review of these
53 factors, we found that while other more traditional factors have been well studied, there is still
54 a lack of characterisation of soil microscale and mesoscale structures and their influence on
55 effective thermal conductivity. In addition, after reviewing the models available in the literature
56 for soil effective thermal conductivity prediction, it was found that compared with empirical
57 and theoretical models, machine learning models can account for the influence of multi-scale
58 factors, however, research into them is scarce. To overcome the limitations of previous
59 research, we proposed a framework that can investigate the factors influencing soil effective
60 thermal conductivity at multiple scale. It includes the impact of soil structural factors at micro
61 to mesoscale, and this impact is integrated with the influence from other factors for accurate
62 thermal conductivity prediction.

63 **Keywords**

64 Soil thermal conductivity; Influencing factors; Prediction models; Soil fabric; Microstructures

65 1 Introduction

66 Heat transfer in geomaterials (soils and rocks) plays an essential role in the geotechnical and geology-
67 engineering applications that contribute to a sustainable development, for example, hydrocarbon
68 exploration (Schimmel et al. 2019), geothermal energy utilisation (Brandl 2006; Jia et al. 2019), thermal
69 energy storage (Bauer et al. 2013), and carbon dioxide sequestration (Fei et al. 2015). Therefore, a clear
70 and updated understanding of the heat transfer behaviour in geomaterials is of utmost importance to
71 improve the reliability and productivity of associated engineering projects.

72 Soil is usually regarded as granular and composite material, and it mainly consists of solid particles and
73 voids. The solid particles are made up of minerals or organic matters; and the voids are usually filled
74 with water or air. Similarly, rocks can be thought as (mildly to highly) cemented granular materials,
75 this is particularly true for sedimentary rocks. Consequently, there are three mechanisms driving heat
76 transfer in soil: a) thermal conduction – heat is transferred from one solid particle to another if two
77 particles contact each other (or through the solid cementation between them); b) thermal convection –
78 the heat transference happens in the voids that contain water or air; and c) thermal radiation – heat
79 transfer between different components and through electromagnetic waves at high temperature
80 (Asakuma et al. 2014). Thermal conductivity (λ) is the property that indicates materials ability to
81 transfer heat, and the λ of different soil constituents varies. In particular, the λ of solid particles is of
82 different magnitude compared with that of water or air in the voids (Yun and Santamarina 2008). For
83 example, $\lambda_{minerals} > 3 \text{ W/(m}\cdot\text{K)}$, $\lambda_{water} = 0.56 \text{ W/(m}\cdot\text{K)}$, $\lambda_{air} = 0.026 \text{ W/(m}\cdot\text{K)}$ at room temperature
84 and atmospheric pressure. Considering the three heat transfer mechanisms in soil and the variation of λ
85 between different components, the *effective* thermal conductivity λ_{eff} is adopted to indicate the overall
86 heat transfer ability. Therefore, studying and predicting λ_{eff} is crucial in understanding soil heat transfer
87 behaviour.

88 The soil λ_{eff} is controlled by soil structure, which can be quantified at different scales: macroscale,
89 mesoscale, and microscale. *Macroscale* structures are derived from regarding different phases in soil as
90 a corresponding whole unit, while ignoring, for example, the connection between solid particles and
91 particles shape and size. For instance, porosity is a macroscale parameter, and it is defined as the ratio
92 of the volume of voids to the total volume of soil. Porosity is mostly used to predict the λ_{eff} because it
93 controls the contribution of different heat transfer mechanisms (e.g., heat conduction or heat convection)
94 to overall λ_{eff} (Yun and Santamarina 2008; Côté and Konrad 2005; Rizvi et al. 2020c). A number of
95 studies have investigated the soil λ_{eff} based on macroscale factors and corresponding models have been
96 proposed to predict the λ_{eff} (Zhang et al. 2017; Zhang and Wang 2017). *Mesoscale* structures involve
97 different particles in soil and characterise the connectivity between them and/or their interrelations with
98 the pore space. For example, particle connectivity, defined by network features based on complex
99 network theory (Fei et al. 2019b), indicates thermal conduction skeleton in soil. *Microscale* structures
100 focus on individual particles. They include information about particle size and shape, which control
101 inter-particle contact area and are defined through parameters like roundness and sphericity (Hryciw et
102 al. 2016; Lee et al. 2017; Fei et al. 2019a). Therefore, investigating the effect of factors at different
103 scales on λ_{eff} is the key to comprehensive understanding of soil heat transfer behaviour. Nevertheless,
104 effects of multiscale (from micro to mesoscale) structural parameters on λ_{eff} have not been
105 comprehensively reviewed and summarised. Furthermore, emerging models (e.g., machine learning
106 models) for soil λ_{eff} prediction have not been included in the previous review papers.

107 This article first reviews the relationship between soil λ_{eff} and various influencing factors at different
108 scales with comprehensive supporting data from the literature. The factors that have not been fully
109 researched yet are summarised. The soil λ_{eff} prediction models that involve different factors are
110 assessed and their potential limitations are identified. To conclude, a research framework is proposed
111 and demonstrated for investigating soil λ_{eff} through factors at multiple scales.

112 2 Influencing factors of effective thermal conductivity

113 For comprehensive review of all influencing factors, a detailed category including non-redundant
114 factors is required, particularly when considering soil structure at different scales. A comparison
115 between the categories in literature and the category adopted in this study is given. Based on the
116 proposed category, the influence of each factor on λ_{eff} is then analysed.

117 2.1 Categories of influencing factors

118 2.1.1 *Categories of influencing factors in literature*

119 The factors influencing soil λ_{eff} have been categorised differently in the various studies. Table 1
120 summarises the methods in the literature to categorise those factors. The classification – compositional
121 factors, environmental factors and other factors – was adopted in (Zhang and Wang 2017); however,
122 this classification could be clearer if compositional factors are further divided into components and
123 structures. Dong et al. (2015) divided the factors into soil constituent, soil type, water content and
124 particle contact; but these categories were redundant, because soil constituent and soil type are
125 correlated. Soil nature, soil structure and soil physical condition were three groups identified by Jin et
126 al. (2017), whereas these groups were not independent either. Abu-Hamdeh (2003) broadly classified
127 the factors influencing soil λ_{eff} into those inherent to soil itself and those can be managed or controlled;
128 but this classification is too general to arrange all the specific influencing factors.

129 2.1.2 *Categories of influencing factors in this study*

130 To address the limitations of previous research in categorising the factors influencing soil λ_{eff} (Zhang
131 and Wang 2017; Dong et al. 2015; Jin et al. 2017; Abu-Hamdeh 2003), this study classify those factors
132 into three types: components properties, structures and environmental conditions, as presented at the
133 bottom of Table 1. The “components properties” consist of the thermal conductivity of the solid material
134 and that of the void typically filled with air or water. The “structures” are considered at three scale
135 levels: macro-level, meso-level and micro-level. Macroscale factors describe the material as a whole,
136 for example, porosity is regarded as a structural factor at macro-level. Mesoscale factors involve two or
137 more particles, for example, particle connectivity belongs to the meso-level. The microscale structural
138 factors, which are based on individual particles, comprise particle shape, particle size and interparticle
139 contact area. In addition, environmental conditions are composed of temperature, density, pressure, and
140 moisture content – these are all macroscale factors as well.

141 *Table 1 Categories of the factors influencing soil effective thermal conductivity*

References	Categories	Factors	Limitations
Zhang and Wang (2017)	Compositions	Mineral components; gradation; particle size and shape; interparticle physical contact, e.g., the number of contact points; change of soil structure during drying and wetting cycle;	Particle connectivity and particle contact area are not arranged properly
	Environmental conditions	Water content and movement; density; temperature;	
	Other	Properties of soil; ions, salts and additives; hysteresis	
Dong et al. (2015)	Constituent	Particle thermal conductivity; mineralogy	The categories are correlated: the soil constituent differences are due mainly to different soil type
	Soil type	Mineral; gradation; particle size and shape	
	Water content Particle contact	Coordination number	
Jin et al. (2017)	Soil nature	Texture; mineralogy; particle shape and size	The categories are not independent: soil particle size and shape are classified into soil nature, but they impact the soil structures
	Structural condition	Porosity; particle arrangement	
	Physical condition	Water content; temperature; pressure	
Abu-Hamdeh (2003)	Factors inherent to soil itself	Mineralogy; composition;	The categories are too general to arrange all specific influencing factors
	Factors manageable	Water content; density; porosity	
This study	Components properties	Particle / air / water thermal conductivity; materials' elastic stiffness	
	Structures	Macro-level: porosity Meso-level: particle connectivity, e.g., coordination number, quantified soil skeleton (Fei and Narsilio 2020) Micro-level: particle size, particle shape, particle contact area	
	Environmental conditions	Temperature; pressure; moisture content	

142 **2.2 Soil components properties influencing the effective thermal conductivity**

143 Heat conduction within particles is an important heat transfer process in geomaterials. Therefore,
144 particle thermal conductivity ($\lambda_{particle}$) influences the soil effective thermal conductivity (λ_{eff})

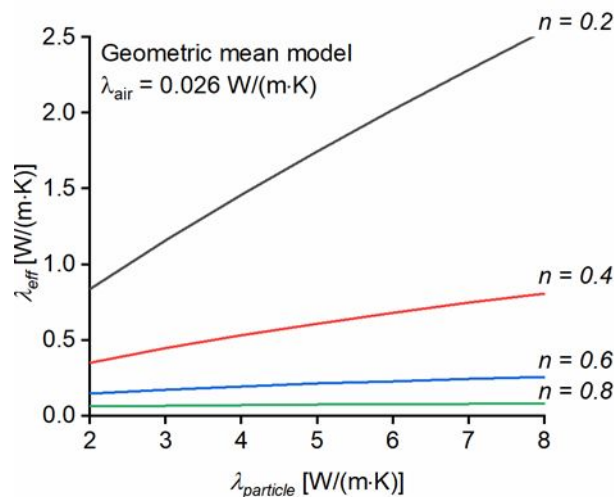
145 (Tarnawski et al. 2009). In general, high soil λ_{eff} could be resulted from high $\lambda_{particle}$ (Côté and Konrad
 146 2005; Zhang et al. 2015b; He et al. 2020). The $\lambda_{particle}$ is determined by the minerals that compose
 147 particles, and it ranges from 1.8 to 8.8 W/(m·K) (He et al. 2020). Johansen (1977) summarised the
 148 thermal conductivity of the minerals at common ambient temperatures around 25 °C, which shows
 149 quartz has the highest thermal conductivity around 7.7 W/(m·K), while mica and feldspar have the
 150 lowest values, both of which are around 2 W/(m·K). Other minerals, e.g., pyroxene, amphibole, olivine,
 151 and chlorite, possess a thermal conductivity ranging from 2 to 5.8 W/(m·K). Consequently, geomaterials
 152 and soils that mainly consist of quartz show a higher λ_{eff} than those composed of other minerals. There
 153 are many models considering $\lambda_{particle}$ for λ_{eff} prediction: series and parallel models by Wiener (1912),
 154 uniform model by De Vries and Van Wijk (1963), geo-mean model by Johansen (1977) and Hashin and
 155 Shtrikman boundary model (Hashin and Shtrikman 1962; Yun and Santamarina 2008). While ignoring
 156 the influence of particle connection and contact on λ_{eff} , they could be used to show the relationship
 157 between λ_{eff} and $\lambda_{particle}$ to some extent. The equation based on geo-mean model (Johansen 1977) is
 158 selected for the showcase considering the available data from He et al. (2020).

$$\lambda_{eff} = \lambda_{particle}^{1-n} \lambda_{water}^{S \times n} \lambda_{air}^{(1-S) \times n} \quad (1)$$

159

$$n = \frac{V_{void}}{V_{total}} \quad (2)$$

160 where $\lambda_{particle}$ is the particle thermal conductivity; λ_{water} is the water thermal conductivity; λ_{air} is the
 161 air thermal conductivity; n is porosity defined as the ratio of void volume V_{void} and total volume V_{total} ;
 162 and S is degree of saturation (the ratio of water volume to void volume). Measured thermal conductivity
 163 data from Birch and Clark (1940) shows that λ_{eff} prediction error using this model is within 20%
 164 (Johansen 1977). Figure 1 exemplifies the influence of $\lambda_{particle}$ on soil λ_{eff} in dry conditions, assuming
 165 $\lambda_{air} = 0.026$ W/(m·K). The figure shows the $\lambda_{particle}$ affects λ_{eff} to a larger extent in soil with low
 166 porosity than in soil with relatively high porosity.



167

168 *Figure 1 Influence of solid particle thermal conductivity $\lambda_{particle}$ on soil effective thermal conductivity λ_{eff} under*
 169 *different porosity based on data from He et al. (2020)*

170 In addition to the solid particle thermal conductivity, elastic stiffness is another component property
 171 that affect the effective thermal conductivity (Morimoto et al. 2022). Morimoto et al. (2022)
 172 investigated the relationship between the thermal conductivity and granular materials' Young's
 173 modulus via the combination of DEM-generated granular samples and corresponding heat pipe network

174 model. According to their findings, soil effective thermal conductivity may increase with its Young's
175 modulus.

176 2.3 Soil structures influencing the effective thermal conductivity

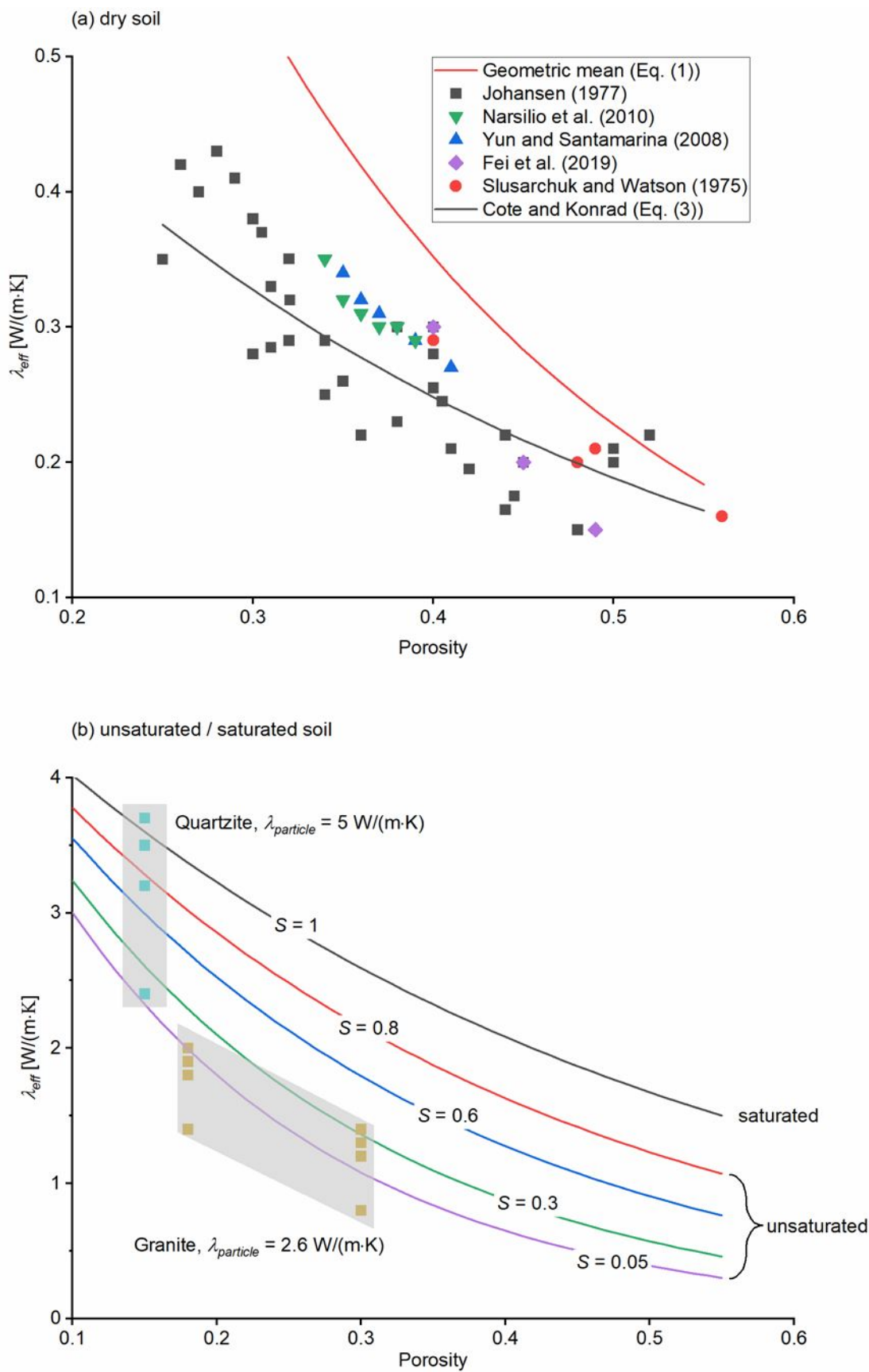
177 2.3.1 Structural feature at macroscale

178 Porosity n is one of soil properties at macro-level and it refers to the fraction of pore volume V_{void} of
179 total volume V_{total} as defined in Eq. (2) above. It is commonly used to describe the macro-structure of
180 granular and sandy soils (Ding et al. 2023) and selected as a key/sole structural feature when
181 establishing predictive models of thermal conductivity (Johansen 1977; Côté and Konrad 2005; Tong
182 et al. 2009; Rizvi et al. 2020a). The void usually contains water and air. Since the values of particle
183 thermal conductivity ($\lambda_{particle}$), water thermal conductivity (λ_{water}) and air thermal conductivity (λ_{air})
184 have different magnitudes and they together determine the soil effective thermal conductivity (λ_{eff}) to
185 some extent, the porosity n influences the soil λ_{eff} remarkably .

186 Porosity is a result of soil texture and particle distribution. Sandy soil has a porosity range from 0.35 to
187 0.5, while finer soil porosity typically ranges from 0.4 to 0.6. Compacted soil possesses a porosity as
188 low as 0.25 to 0.3 (Carter and Gregorich 2007). Overall, soil λ_{eff} decreases with the increase of porosity
189 (Côté and Konrad 2005). Figure 2(a) shows the change of dry soil λ_{eff} with porosity. The included data
190 are collected from Slusarchuk and Watson (1975); Johansen (1977); Côté and Konrad (2005); Yun and
191 Santamarina (2008); Narsilio et al. (2010); Fei et al. (2019b). Soil λ_{eff} in dry conditions ranges from
192 about 0.15 to 0.45 W/(m·K) while the porosity changes from about 0.25 to 0.55. Furthermore, Côté and
193 Konrad (2005) claimed that dry soil λ_{eff} is directly related to porosity and they proposed the following
194 exponential relationship between the two parameters:

$$\lambda_{eff, dry} = \chi \cdot 10^{-\eta n} \quad (3)$$

195 where $\lambda_{eff, dry}$ is the effective thermal conductivity of dry soil; χ and η are coefficients related to soil
196 particle shape. They applied the equation to various soils: χ and η are 0.75 W/(m·K) and 1.2 for natural
197 mineral sands, 1.7 W/(m·K) and 1.8 for crushed rocks, 0.3 W/(m·K) and 0.87 for organic fibrous soil.
198 Figure 2(b) shows the change of unsaturated and saturated soil λ_{eff} with porosity. The experimental
199 data for quartzite and granite are from Côté and Konrad (2005). It indicates that the porosity affects
200 λ_{eff} to a larger extent with high degree of saturation, S , than low degree of saturation.



201

202 *Figure 2 The distribution of soil effective thermal conductivity λ_{eff} with porosity: (a) dry soils with data from*
 203 *Slusarchuk and Watson (1975); Johansen (1977); Côté and Konrad (2005); Yun and Santamarina (2008);*
 204 *Narsilio et al. (2010); Fei et al. (2019b); χ and η are 0.75 W/(m·K) and 1.2 for generating Eq. (3); $\lambda_{particle}$, λ_{air}*

Can. Geotech. J. Downloaded from cdnsciencepub.com by UNIVERSITY OF MELBOURNE on 04/08/24
 For personal use only. This Just-IN manuscript is the accepted manuscript prior to copy editing and page composition. It may differ from the final official version of record.

205 and S are $2 \text{ W/(m}\cdot\text{K)}$, $0.026 \text{ W/(m}\cdot\text{K)}$ and 0 for generating Eq. (1); (b) unsaturated / saturated soils predicted
 206 values using Eq. (1) with $\lambda_{\text{particle}}=5 \text{ W/(m}\cdot\text{K)}$, $\lambda_{\text{water}}=0.56 \text{ W/(m}\cdot\text{K)}$, $\lambda_{\text{air}}=0.026 \text{ W/(m}\cdot\text{K)}$; quartzite and granite
 207 experimental data is from Côté and Konrad (2005)

208 2.3.2 Structural features at mesoscale

209 Particle connectivity indicates soil skeleton and thus relates to the pathways of heat conduction between
 210 particles. Since heat conduction between particles dominates the heat transfer processes in soil, particle
 211 connectivity is important to soil effective thermal conductivity λ_{eff} (Dong et al. 2015). However, the
 212 indices of soil particle connectivity have not been well studied. Cheng et al. (1999) described the particle
 213 connectivity based on the results measured by Finney (1970), but only mono-sized spheres were
 214 considered. Particle connectivity could also be obtained if employing Discrete Element Modelling
 215 (DEM) for granular assemblies, since the contact between discrete particles and packing characteristics
 216 of granular systems can be found within DEM. Although research has been conducted on heat transfer
 217 using DEM, those work mainly focused on the computation of effective thermal conductivity and
 218 structural characterisation was out of their scope (Vargas and McCarthy 2001; Feng et al. 2009).
 219 Structural parameters such as packing fraction and macroscopic stress has been investigated by Peeketi
 220 et al. (2019) but further quantification of particle connectivity change due to altered packing and stress
 221 conditions is still missing. Many other studies used coordination number derived from DEM-generated
 222 granular assembly to investigate thermal conductivities (Yun and Evans 2010; El Shamy et al. 2013).
 223 Nonetheless, traditional coordination number alone cannot capture all information of complex granular
 224 materials' structure. For example, traditional coordination number only considers the number of
 225 contacts between particles but ignores the contact quality, which determine the thermal resistance
 226 between particles. Further description and quantification of particle connectivity cannot be achieved
 227 without other theories and tools.

228 Fei and Narsilio (2020); Fei et al. (2020) used complex network theory to characterise soil particle
 229 connectivity based on X-ray computed tomography (CT) images. To use complex network theory to
 230 characterise soil particle connectivity, a network representing soil particles has to be built first based on
 231 real soil CT images. This network's format is similar to that studied in (Feng et al. 2009; Yun and Evans
 232 2010; El Shamy et al. 2013; Morimoto et al. 2022): soil is represented as a web composed of nodes and
 233 edges; the nodes represent individual particles, and edges exist between contacted particles. Then, the
 234 complex network theory can be applied to the built network to extract structural features. These
 235 structural features provide more comprehensive indices for particle connectivity and soil structure
 236 quantification, and these indices are classified into four types: centrality, network scale, cycles and
 237 clustering, as listed in Table 2. These different types describe structures of a soil particle assembly via
 238 different aspects (Newman 2003). The "centrality" type quantifies the importance of nodes (particles)
 239 within a network (granular assembly) based on their position or the number of paths passing through
 240 them. For example, the *degree* of a node in a network is the number of edges linked to this node, which
 241 is equivalent to coordination number in soil mechanics and powder technology. *Closeness centrality* of
 242 a node measures the how closely this node is related to other nodes, as exemplified in Figure 3 and
 243 detailed in Table 2. *Betweenness centrality* measures how often a node appears on the shortest path
 244 between two other nodes. The "network scale" measures the network size and interactions between
 245 nodes encompassed in a network. For example, *network diameter* is equal to the length of the longest
 246 one among the shortest paths between any two nodes in a network, as illustrated in Figure 3. The "cycle"
 247 type indicates the loop starting and ending at the same node and thus 3-cycles represent triangles. The
 248 "clustering" type measures the tendency of nodes to form tightly-knit groups or communities within a
 249 larger network as detailed in Table 2 and Figure 3.

250 Furthermore, weighted networks are established by adding contact area or thermal conductance as the
 251 weight to network edges, resulting in new weighted sub-indices under each type. In an unweighted
 252 network, an edge only indicates two nodes are connected. Even though the edges in Figure 3 have
 253 different lengths, the lengths have not been considered as weight for the edges. For network representing

254 granular soils, if the contact area between two particles in physical contact is used to weight the edge
 255 between two nodes that represent those two particles in a network, the length of this edge has a physical
 256 meaning of the contact area. This process of adding weights to edges in a network bring physical
 257 meanings to the network features, and consequently the network features account for not only the
 258 number of particles contacts but also the contact quality. The influence from contact area / thermal
 259 conductance-weighted network features on heat transfer is also included in Table 2.

260 In general, soil λ_{eff} correlates directly proportional to the degree (also known as coordination number
 261 in soil mechanics and powder technology). For closeness centrality, soil λ_{eff} is related to the weighted
 262 value directly proportional while the unweighted value inversely proportional. Besides, soil λ_{eff}
 263 decreases with the increase of the betweenness centrality. In terms of network scale indices, soil λ_{eff} is
 264 inversely correlated to the average weighted shortest path. As for cycles and clustering, λ_{eff} increases
 265 with the number of 3-cycle in a network. Particularly, the weighted degree and weighted closeness
 266 centrality are identified as the best predictors for soil λ_{eff} (Fei and Narsilio 2020). A quantitative
 267 relationship between soil λ_{eff} and network features is given below (Fei et al. 2020) :

$$\frac{\lambda_{eff}}{\lambda_{solid}} = -0.21([G^C]_{\kappa_w})^2 + 0.67[G^C]_{\kappa_w} + 0.25 \quad (4)$$

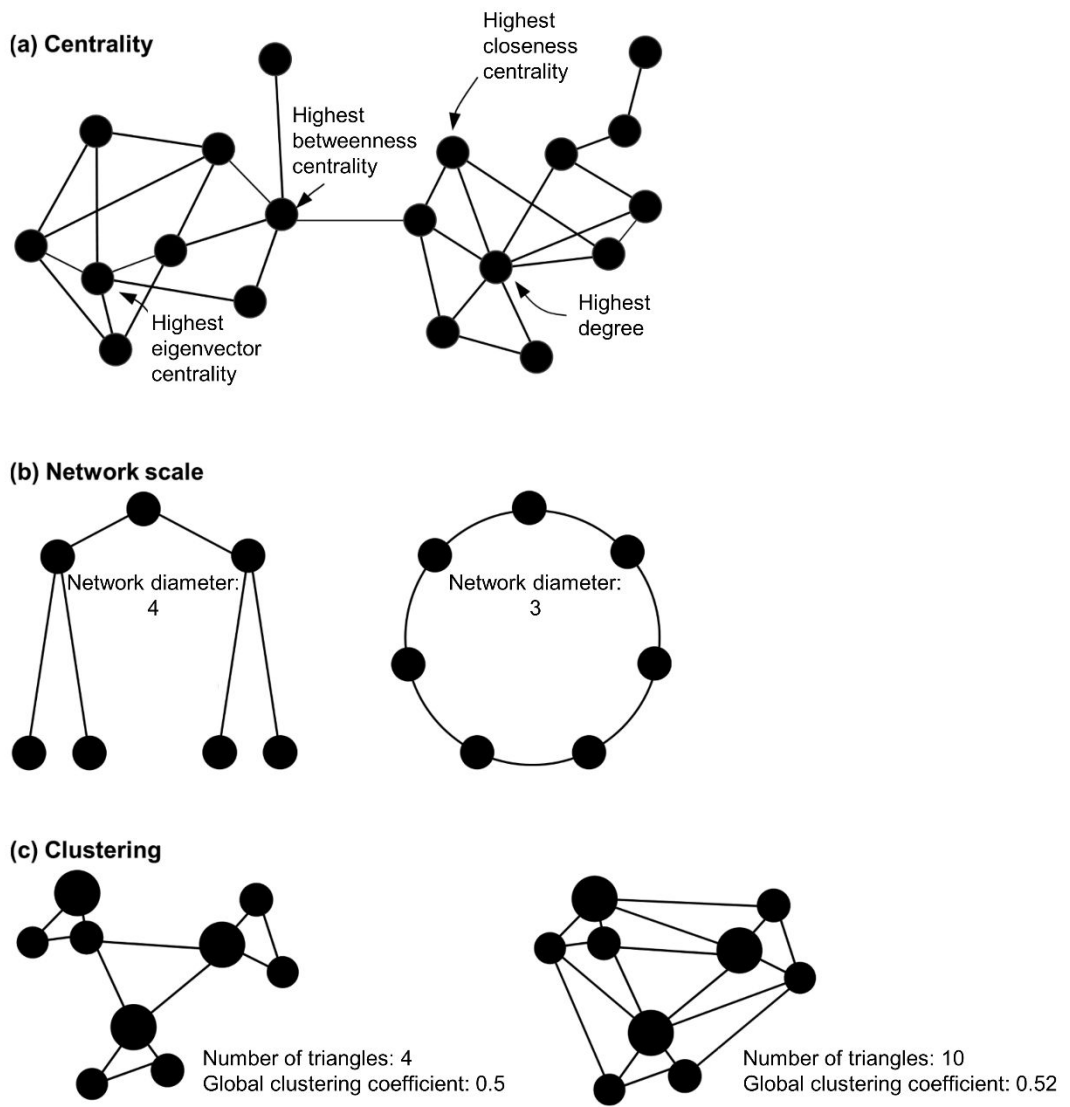
268 where λ_{solid} is the solid particle thermal conductivity; $[G^C]_{\kappa_w}$ is the *degree* weighted by the contact area
 269 between particles. Figure 4 illustrates the influence of *weighted degree* on soil λ_{eff} for different sands
 270 with data from Fei et al. (2021). The complex network methodology for soil structure quantification has
 271 not been extended to unsaturated soil, where water fills voids and bridges particles, and hence updated
 272 networks need to be proposed for studying heat transfer in unsaturated soil.

273 *Table 2 Indices of soil particle connectivity at mesoscale based complex network theory and their relationship with soil effective thermal conductivity λ_{eff} (Fei and Narsilio*
 274 *2020; Fei et al. 2020)*

Type	Sub-indices	Description	Correlation with λ_{eff}
Centrality	Degree*	The number of edges linked to a node	Directly proportional
	Closeness centrality*	Related to distance of a node to other nodes and defined as $[G]_C(i) = \beta \left[\sum_{j=1}^{ V } d(i,j) \right]^{-1}$; $[G]_C(i)$ is closeness centrality of node i ; β is a normalisation term; V is a node-set including i and j ; $d(i,j)$ is the shortest path length from i to j .	Directly proportional for weighted values but inversely proportional for unweighted values
	Betweenness centrality*	Related to the extent that a node or edge connects other nodes or edges: $[G]_B(i) = \beta \sum_{j,k \in V} \frac{\sigma(j,k i)}{\sigma(j,k)}$; $[G]_B(i)$ is betweenness centrality of node i ; β is a normalisation term; $\sigma(j,k)$ is the number of $d(j,k)$; $\sigma(j,k i)$ is number of $d(j,k)$ passing the node i .	Inversely proportional
Network scale	Eigenvector centrality*	The contribution of a node to network connectivity	
	Network diameter	The longest one among the shortest length paths: $[G]_D = \text{Max}_{i,j \in V} [d(i,j)]$; $[G]_D$ is network diameter; V is the node set included in the network; $d(i,j)$ is the shortest path length from node i to node j .	
	Average shortest path length*	The average of the shortest length paths from every node to other nodes.	Inversely proportional
	Network density	The ratio of actual edge number to potential edge number	
Cycles	Number of 3-cycle	Number of loops in a network that starts and ends at the same node and has 3 edges	Directly proportional
Clustering	Global clustering coefficient	Indicating how integrated or fractured the network is: $G_{GC} = 3 \frac{\text{triangles' number}}{\text{connected triples' number}}$	

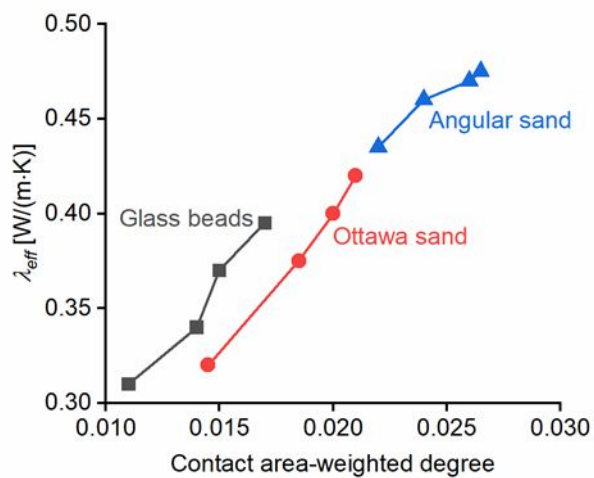
Type	Sub-indices	Description	Correlation with λ_{eff}
		G_{GC} is the global clustering coefficient; a 'triangle' is a three nodes-set connected by three edges; a 'triple' is a three nodes-set connected by three / two edges .	
	Local clustering coefficient*	$[G]_{LC}(i) = \frac{2T(i)}{\kappa(i)[\kappa(i) - 1]}$, $[G]_{LC}(i)$ is the local clustering coefficient of node i ; $T(i)$ is the number of triangles passing node i ; $\kappa(i)$ is the degree of node i .	

275 * For the sub-indices calculated based on individual node or edge, the average value is adopted. The asterisk * indicates an average value.



276

277 *Figure 3 Network features illustration based on complex network theory from (Fei and Narsilio 2020)*



278

279 *Figure 4 Influence of contact area-weighted degree in complex network theory on soil effective thermal*
 280 *conductivity λ_{eff} in with data from Fei et al. (2021)*

281 2.3.3 Structural features at microscale

282 Soil particle shape and size control the contact area between particles, and the contact area governs the
 283 heat conduction process in soil. Since heat conduction between particles dominates the heat transfer
 284 processes in soil, particle shape and size are the key factors that influence soil effective thermal
 285 conductivity λ_{eff} (Gan et al. 2017; Lee et al. 2017; Fei et al. 2019a). Many studies adopt coefficients
 286 rather than particle shape and size descriptors themselves to consider the effect (De Vries 1963; Côté
 287 and Konrad 2005), where a quantitative relationship between λ_{eff} and particle shape and size is missing.
 288 To quantify the particle size and shape influence, this section firstly reviews the methods for particle
 289 size and shape description.

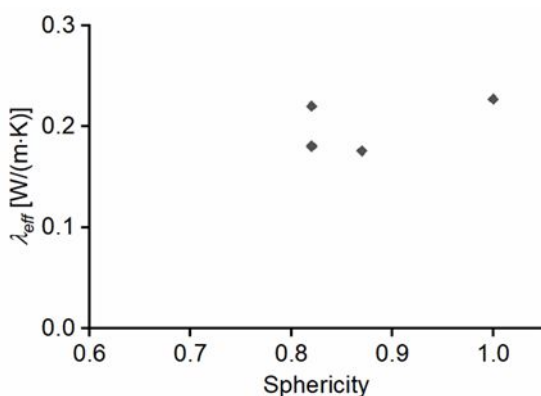
290 Two-dimensional microscopic images-based descriptors for particle shape, such as circularity,
 291 sphericity, roundness, etc., have been introduced in Cherkasova and Shan (2008); Cox and Budhu
 292 (2008); Lee et al. (2017) and (Xiao et al. 2020); however, they have some limitations when
 293 characterising irregular particles in natural soil, because the derived descriptor values may vary with
 294 the directions of projections (Fei et al. 2019a). Three-dimensional sphericity is introduced and used in
 295 Wadell (1932); Hamilton and Crosser (1962); Verma et al. (1991). Sphericity in these studies is defined
 296 as $\frac{\text{Surface area of volume equivalent sphere}}{\text{Surface area of actual particle}}$. Nevertheless, elongated particles cannot be well described using
 297 this definition. Lees (1964) described the angularity of particles using three main features: number of
 298 corners, corners degree of projection, and corners degree of acuteness. Zhou et al. (2018) combined
 299 roundness and sphericity to describe real sand particles with different shapes. Volume-based aspects
 300 ratio was found to have a positive correlation to thermal conductivity of silver nanofluids
 301 (Mirmohammadi et al. 2019). More recent works use sphericity in Eq. (5) and roundness in Eq. (6) for
 302 particle shape representation (Fei et al. 2019a). These two descriptors can be computed using CT images
 303 of real soil particles.

$$304 \text{ Sphericity} = \frac{36\pi V^2}{(SA)^3} \quad (5)$$

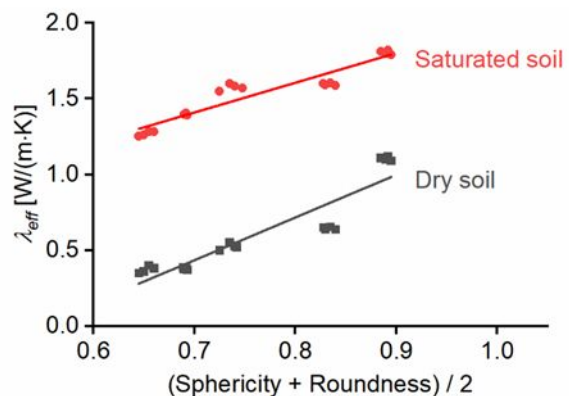
$$305 \text{ Roundness} = \frac{\sum \frac{r_i}{N}}{r_{\max, in}} \quad (6)$$

304 where V is particle volume and SA is particle surface area in Eq. (5); r_i is the radius of the i^{th} particle
 305 corner, N is the number of particle corners and $r_{\max, in}$ is radius of the maximum inscribed sphere in Eq.
 306 (6). Figure 5 shows the soil λ_{eff} change with different particle shape. In general, soil composed of
 307 spherical and round particles has a higher λ_{eff} than that composed of elongated and angular particles.

(a) $\text{Sphericity} = \frac{\text{Surface area of equivalent volume sphere}}{\text{Surface area of actual particle}}$



(b) Sphericity and roundness defined by Eq. (5) & (6)

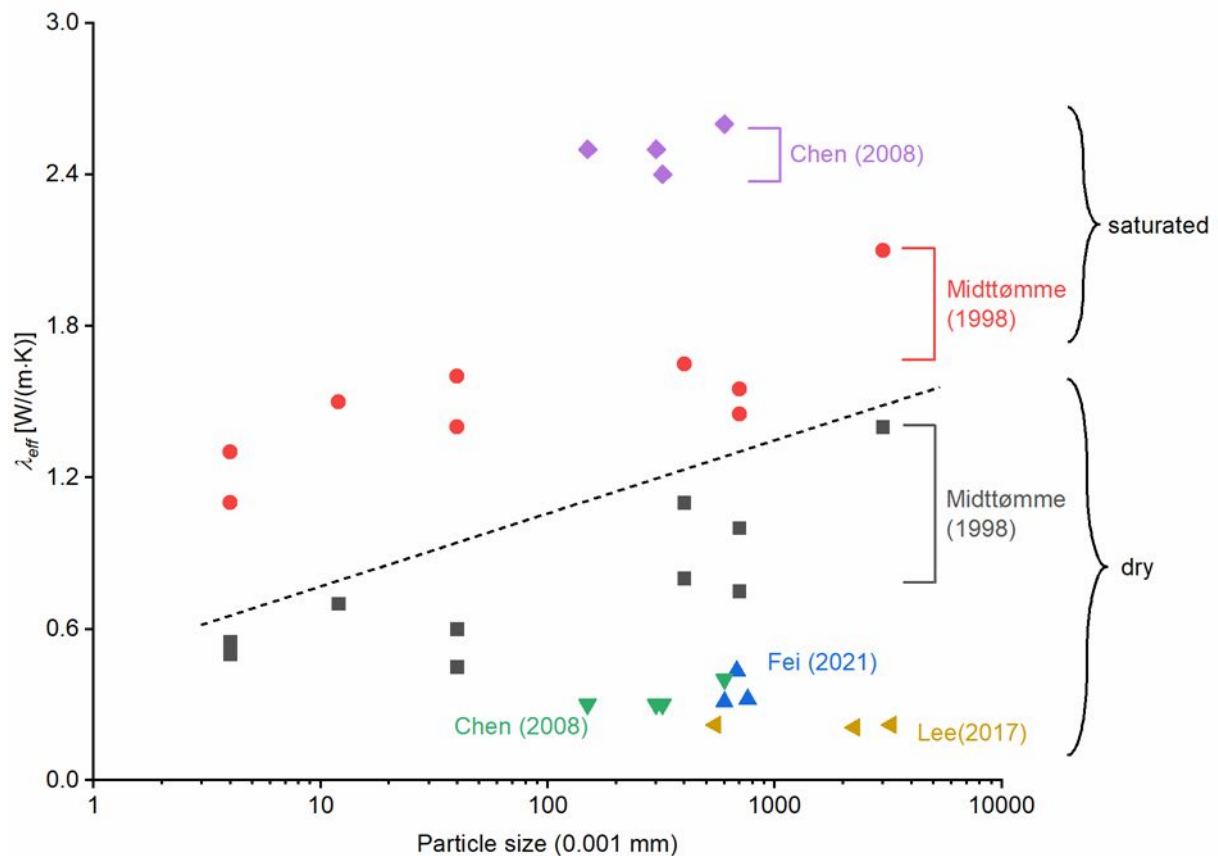


308

309 *Figure 5 Influence of particle shape on soil effective thermal conductivity λ_{eff} (a) shape defined by surface areas*
 310 *with dry glass experimental data from Verma et al. (1991); λ_{solid} is around $1 \text{ W}/(\text{m} \cdot \text{K})$, λ_{air} is around*
 311 *$0.025 \text{ W}/(\text{m} \cdot \text{K})$; (b) shape defined by Eq. (5) and Eq. (6) with data from Fei et al. (2019a); λ_{solid}*
 312 *$= 3 \text{ W}/(\text{m} \cdot \text{K})$, $\lambda_{air} = 0.025 \text{ W}/(\text{m} \cdot \text{K})$, $\lambda_{water} = 0.591 \text{ W}/(\text{m} \cdot \text{K})$*

313 Parameters including 1) the fraction of relatively large particles in soil assembly and 2) particle mean
 314 or median diameters are usually used to study the influence of particle size on soil λ_{eff} . In most cases,
 315 soil with a larger particle size shows a higher λ_{eff} than that with smaller particle size (Zhang et al.
 316 2015a; Gan et al. 2017). Gan et al. (2017) argued that small particle size leads to less particle contact
 317 area, and thus reduces the heat conduction between particles and lowers effective thermal conductivity
 318 in dry condition. It should be noted that, however, for unsaturated soil, small particle size leads to high
 319 soil λ_{eff} (Zhang et al. 2015b). This is because small particle size results in large surface area, and thus
 320 water films and bridges are easily formed between particles, thereby reducing thermal resistance
 321 considering that water has a greater ability for heat transfer than air. Furthermore, compared with the
 322 λ_{eff} of soil with low particle thermal conductivity, the λ_{eff} of soil with high particle thermal
 323 conductivity is more easily influenced by particle size (Zhou et al. 2010; Gan et al. 2017). Figure 6
 324 presents general relationship between soil λ_{eff} and particle size. Mean particle diameters are used by
 325 Midttomme and Roaldset (1998), where particles are derived from synthetic samples with relatively
 326 uniform particle size. Median particle diameters are used by Fei et al. (2021), Lee et al. (2017) and Chen
 327 (2008), where diameters are from sieve analysis. The λ_{eff} relates more closely with mean diameters
 328 than median diameters.

329



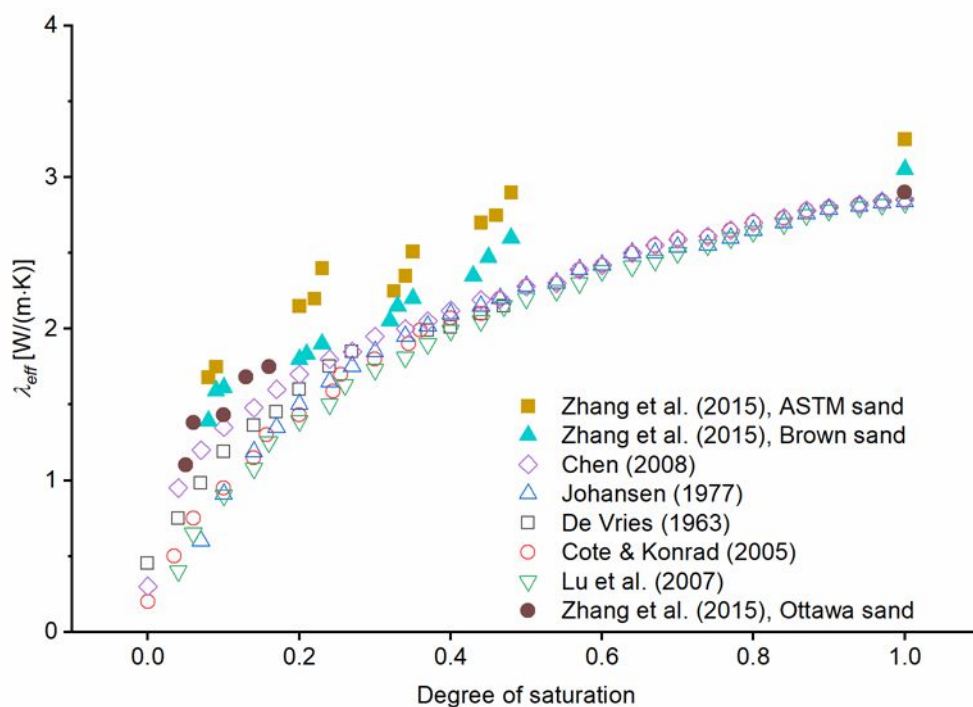
330

331 *Figure 6 Influence of particle size on soil effective thermal conductivity λ_{eff} with data from Midttomme and*
 332 *Roaldset (1998); Chen (2008); Lee et al. (2017); Fei et al. (2021)*

333 2.4 Environmental conditions influencing the effective thermal conductivity

334 2.4.1 Soil water content

335 The pores around solid particles in soil are typically filled with either air or water. Since water can
 336 reduce the thermal resistance between particles remarkably (Rao and Singh 1999), the water content,
 337 or more precisely the degree of saturation S (the ratio of water volume to voids volume) and volumetric
 338 moisture content θ (the ratio of water volume to soil volume) are considered as the prominent factors
 339 that affect soil effective thermal conductivity λ_{eff} (Zhang and Wang 2017; Agrawal et al. 2019; Lu and
 340 Dong 2015). Some studies report gravimetric moisture content w (the ratio of water mass to soil mass)
 341 rather than S and θ . In general, soil λ_{eff} under unsaturated or fully saturated conditions is higher than
 342 that under dry conditions (Johansen 1977; Chen 2008). Moreover, the soil λ_{eff} grows more rapidly at
 343 low S or θ compared with that at high S or θ (Zhang et al. 2015b; Dong et al. 2015). At low S or θ ,
 344 solid particle connections are established gradually by water bridges formed in the voids. Considering
 345 thermal conductivity of water is greater than of air, these connections facilitate heat conduction in soil
 346 thereby increasing the soil λ_{eff} . In contrast, at high S or θ moisture content, solid particles are almost
 347 fully connected by water bridges so the soil λ_{eff} grows slightly. Moreover, the influence of water
 348 bridges depends on the void volume. Considering w is not as related to the void volume as S and θ , S
 349 and θ could be indicators that truly and generally influence λ_{eff} . Lu and Dong (2015) further introduced
 350 S_f and θ_f , at which the rate of change in thermal conductivity reaches maximum, for predicting soil
 351 λ_{eff} . Figure 7 shows the relationship between soil λ_{eff} and S with predicted values from De Vries
 352 (1963), Johansen (1977), Côté and Konrad (2005), Lu et al. (2007), Chen (2008), and experimental data
 353 from Zhang et al. (2015b).



354

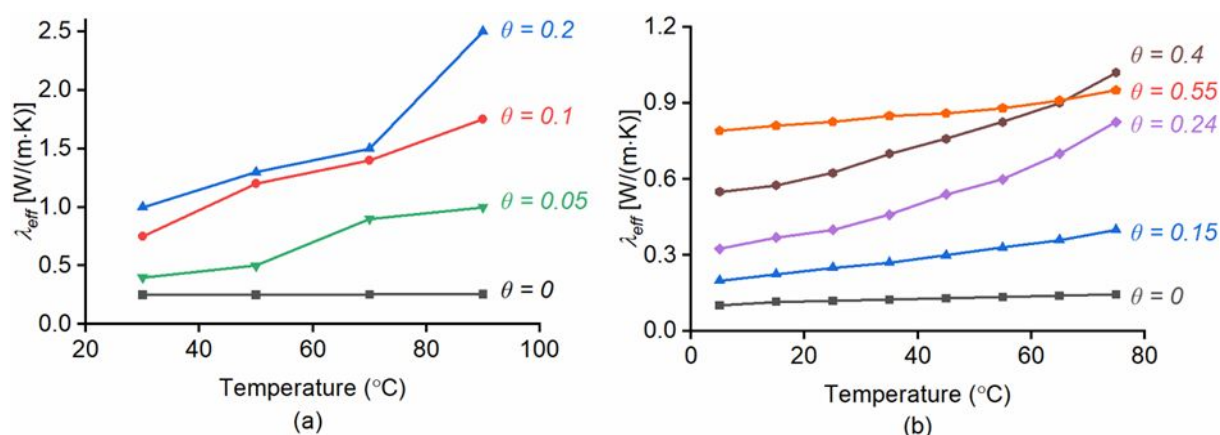
355 *Figure 7 Influence of degree of saturation on soil effective thermal conductivity λ_{eff} with data from De Vries*
 356 *(1963); Johansen (1977); Côté and Konrad (2005); Lu et al. (2007); Chen (2008); Zhang et al. (2015b)*

357 2.4.2 Soil temperature

358 Soil temperature influences the thermal conductivity of soil components, i.e., soil particles, air and
 359 water (Kayaci and Demir 2018). Besides, temperature can result in components phase change in soil
 360 and thus change the soil effective thermal conductivity (Gori and Corasaniti 2002). For example, under
 361 temperature below freezing point, part of fluid water in soil changes into solid ice, whose thermal

362 conductivity is different from that of fluid water. The effects of temperature ranging from 30 °C to 90 °C
 363 are reviewed here. This temperature range is mostly encountered in shallow geothermal engineering,
 364 disposal of radioactive waste and thermal remediation of contaminated soils. In general, soil λ_{eff} rises
 365 with temperature, and its value at 90 °C is three to five times of that at ambient temperature (Campbell
 366 et al. 1994). This is attributed to latent heat transfer, caused by evaporation of water in soil voids, under
 367 high temperature and pressures different from atmospheric pressure (Liu et al. 2011). Furthermore, soil
 368 λ_{eff} increases more noticeably with temperature above 50 °C compared with that ranging from 30 to 50
 369 °C (Smits et al. 2013), and temperature effect is negligible below 30 °C (Lu and Ren 2009). Besides, the
 370 impact of temperature on λ_{eff} is greater in moist soil than in dry soil, and it is most obvious when the
 371 soil degree of saturation is between 22% to 50% (Sepaskhah and Boersma 1979). Figure 8 visualizes
 372 the influence of temperature on soil λ_{eff} under different volumetric water content.

373



374

375 *Figure 8 Influence of temperature on soil effective thermal conductivity λ_{eff} with experimental data selected from*
 376 *(a) quincy sand at different volumetric water content (Campbell et al. 1994) and (b) clay loam at different*
 377 *volumetric water content (Hiraiwa and Kasubuchi 2000)*

378 2.4.3 Soil loading and gradation

379 Soil loading refers to the external forces acting on the soil beside self-weight. Soil loading induces
 380 compression thus increases the particle contact area between particles, as well as reducing porosity.
 381 Therefore, increasing loading increases the heat conduction process in soil and influences the soil
 382 effective thermal conductivity λ_{eff} . The λ_{eff} variation should also be attributed to the stress
 383 heterogeneity resulted from soil loading (Vargas and McCarthy 2001). Besides, soil structure (e.g.,
 384 porosity, density, and particle connectivity) changes under loading, and consequently the soil λ_{eff}
 385 changes. In general, soil λ_{eff} is positively correlated to soil loading, and it almost increases linearly
 386 with the loadings (Vargas and McCarthy 2001; Weidenfeld et al. 2004). Weidenfeld et al. (2004) studied
 387 the effective thermal conductivity of particle beds composed of glass/limestone/aluminium etc. and
 388 found that λ_{eff} rises with different materials to different extents under compression. This finding should
 389 also be applied to soil considering the similarity between the particle beds and soil packings. Moreover,
 390 the influence of soil loading on λ_{eff} is negligible when the particle thermal conductivity is as low as
 391 less than 1 W/(m·K) (Weidenfeld et al. 2004). Compared with soil with small particle size, the λ_{eff} of
 392 that with large particle size is more easily influenced by the loading (Weidenfeld et al. 2004).
 393 Furthermore, the dependence of soil λ_{eff} on loading increases with the irregularity of particles because
 394 irregularity leads to more sensitive granular skeleton (Yun and Santamarina 2008). Cui et al. (2023)
 395 conducted a series of thermal test for soil specimens under loading-unloading conditions and at various
 396 degree of saturated. It was found that the change of thermal conductivity with loading-induced stress is
 397 more obvious under unsaturated condition compared with that under dry conditions. This effect is
 398 because that the addition of water improves soil suction and thus lowers soil compressibility. The

399 influence of stress on λ_{eff} also depends on soil initial compression state: more loose soil tends to be
 400 more easily affected by stress. In addition, Xiao et al. (2018) studied the dependence of thermal
 401 conductivity on soil gradation, and it was found that thermal conductivity increases with soil uniformity
 402 coefficient.

403 3 Models for effective thermal conductivity prediction

404 After reviewing the influence of various factors on soil effective thermal conductivity λ_{eff} , models
 405 integrating those factors for λ_{eff} prediction are summarised in this section. Models for λ_{eff} prediction
 406 are mainly classified into three types: theoretical models, empirical models, and machine learning
 407 models.

408 Theoretical models are based on conceptual material geometry, and these models assume that different
 409 components in soil, i.e., solid, air, and water, are uniformly distributed. Then, the mathematical
 410 expressions for λ_{eff} are developed (Wiener 1912; De Vries and Van Wijk 1963; Gori 1983; Tong et al.
 411 2009; Haigh 2012; Johansen 1977). Empirical models are proposed through comparing measured λ_{eff}
 412 with the value of different influencing factors (e.g., particle thermal conductivity, porosity, moist
 413 content). From this comparison, the key empirical coefficients that reveal the relationship between λ_{eff}
 414 and various factors can be drawn (Kersten 1949; Johansen 1977; Donazzi et al. 1979; Rao and Singh
 415 1999; Balland and Arp 2005; Côté and Konrad 2005; Lu et al. 2007; Chen 2008). Machine learning
 416 models are based on trustable data and a learning process, which involve mathematic algorithms to
 417 establish the relationship between inputs (influencing factors) and outputs (λ_{eff}) (Grabarczyk and
 418 Furmański 2013; Li et al. 2022a). Table 3 summarises the considered factors and features of each model.

419 3.1 Theoretical models

420 Wiener (1912) defined the lowest and highest value of λ_{eff} by assuming that different phases in soil are
 421 ideally distributed. De Vries and Van Wijk (1963) model is a more complex one compared with Wiener
 422 model. It accounts for particle shape effect on λ_{eff} but the related coefficient is not easy to obtain.
 423 Johansen (1977) proposed a “geo-mean” model with a succinct mathematical expression. Gori (1983)
 424 model focuses on the λ_{eff} under different water distribution regimes and it is complicated to implement.
 425 Tong et al. (2009) model was developed from Wiener model. It is a comprehensive one because the
 426 effects of pore structure, degree of saturation and temperature are considered. Haigh (2012) model
 427 considers water film development (i.e., its width and thickness) when predicting λ_{eff} .

428 3.2 Empirical models

429 The λ_{eff} of soil with different temperatures, degree of saturation and mineral was measured by Kersten
 430 (1949), and he proposed two prediction equations for silts (or clay) and sandy soil respectively. In
 431 addition to the “geo-mean” model, Johansen (1977) also proposed “normalized thermal conductivity
 432 λ_r ”, which is expressed as:

$$433 \lambda_r = \frac{\lambda_{eff} - \lambda_{dry}}{\lambda_{sat} - \lambda_{dry}} \quad (7)$$

434 where λ_{dry} is thermal conductivity under dry conditions, and λ_{sat} is that under saturated conditions.
 435 Johansen developed several relationships between λ_r and degree of saturation S . And λ_r can be used to
 436 estimate λ_{eff} by interpolating λ_{sat} and λ_{dry} . This dimensionless coefficient has already involved many
 437 factors (e.g., soil type, mineralogy) and thus simplifies the prediction and widens the application range
 438 compared with the Kersten (1949) model. Balland and Arp (2005) model has an emphasis on the effect
 439 of organic matters on λ_{eff} . Côté and Konrad (2005) updated the λ_r - S relationship by considering soil
 type effect. Lu et al. (2007) claimed a linear correlation between λ_{eff} and porosity for dry soil. Chen

440 (2008) model has a good accuracy when predicting λ_{eff} of soil with high quartz contents. Other
441 empirical models include Donazzi et al. (1979) model and Rao and Singh (1999) model.

442 3.3 Machine learning models

443 Machine learning models for λ_{eff} prediction are developed based on a large amount of trustable data
444 regarding influencing factors and λ_{eff} (Wei et al. 2018). Typically, their architecture includes three
445 layers: the input layer for influencing factors, the hidden layers for applying weights to the inputs, as
446 well as the output layers for λ_{eff} . They can provide fast and convenient predictions when validated by
447 trustable data.

448 Wei et al. (2018) used three methods: convolutional neural network (CNN), gaussian process regression
449 (GPR) and support vector regression (SVR), to train available data and develop machine learning
450 models. This work proves that machine learning models can provide accurate prediction. SVR and GPR
451 are machine learning methods for non-linear regression analysis; and estimating porous media λ_{eff} from
452 various factors is a non-linear problem. CNN has been widely applied in face recognition and thus it is
453 able to capture the structure information in λ_{eff} prediction. Furthermore, six machine learning
454 algorithms for soil λ_{eff} prediction are investigated in Li et al. (2022b). These algorithms include SVR,
455 GPR, adaptive boosting method (AdaBoost), random forest (RF), decision tree (DT), and multivariate
456 linear regression (MLR). The results show that AdaBoost provides good estimated values with the
457 lowest error. Seven algorithms, including GPR, RF, DT, MLR, gradient boosting decision tree (GBDT),
458 k-nearest neighbours (KNN), artificial neural network (ANN) were compared by Zhao et al. (2022)
459 using different databases from Li et al. (2022b). These studies conclude that GPR, DT, and MLR are
460 not the preferred algorithms for soil λ_{eff} prediction. Moreover, ANN was recommended by Zhao et al.
461 (2022). A screen ANN is used to offset the influence of soil database insufficiency, and it utilises back-
462 propagation algorithm in the training stage (Zhang et al. 2020). In addition, in order to balance the
463 complexity with the accuracy of the prediction model, this study compares the model performances
464 under different combinations of inputs. Rizvi et al. (2020a) developed an ANN model for unsaturated
465 soil λ_{eff} prediction. Different parameters, including porosity, degree of saturation and quartz content,
466 are used as inputs for the model; and the back-propagation algorithm is adopted for calculating the
467 weight values in the ANN hidden layer. The same author also used a ANN based on group method of
468 data handling (GMDH) to predict sand λ_{eff} (Rizvi et al. 2020b). Multilayer perceptron ANN is
469 considered as the optimal one for the prediction of sandstone λ_{eff} (Vaferi et al. 2014). Mesoscale and
470 microscale structures were firstly integrated into the inputs of ANN models in Fei et al. (2021). Inputs
471 in his model consist of particle thermal conductivity, porosity, coordination number, particle roundness
472 and sphericity. In general, machine learning models are able to account for more factors and can be
473 applied to a wide range.

Table 3 Summary of prediction models for soil effective thermal conductivity λ_{eff}

Model category	Author	Expression	Comments	Factors involved in each model											
				λ , thermal conductivity, W/(m·K)			ϕ , volume fraction			n , porosity			S , saturation degree		
				ρ , dry density, kg/m ³			w , gravimetric moisture			T , temperature, °C			C , coefficient		
				λ_{solid}	λ_{water}	λ_{air}	ϕ_{solid}	ϕ_{water}	ϕ_{air}	n	S	ρ	w	T	C
Theoretical models	Wiener (1912)	$\lambda_{eff, lower} = \left[\sum \frac{\phi_{\alpha}}{\lambda_{\alpha}} \right]^{-1}$ $\lambda_{eff, upper} = \sum \phi_{\alpha} \lambda_{\alpha}$ α indicates different phase	Determining the upper and lower boundary of λ_{eff} .	<input checked="" type="checkbox"/>	<input checked="" type="checkbox"/>	<input checked="" type="checkbox"/>	<input checked="" type="checkbox"/>	<input checked="" type="checkbox"/>	<input checked="" type="checkbox"/>						
	De Vries and Van Wijk (1963)	$\lambda_{eff} = \frac{\sum K_{\alpha} \phi_{\alpha} \lambda_{\alpha}}{\sum K_{\alpha} \phi_{\alpha}}$ K_{α} is the ratio of average thermal gradient of each constituent to that of continuous medium in soils	K_{α} is related to particle shape, and position, and it is difficult to be determined.	<input checked="" type="checkbox"/>	<input checked="" type="checkbox"/>	<input checked="" type="checkbox"/>	<input checked="" type="checkbox"/>	<input checked="" type="checkbox"/>	<input checked="" type="checkbox"/>						<input checked="" type="checkbox"/>
	Johansen (1977)	$\lambda_{eff} = \lambda_{solid}^{1-n} \lambda_{water}^S \lambda_{air}^{(1-S)n}$	Developed from Wiener model (1912).	<input checked="" type="checkbox"/>	<input checked="" type="checkbox"/>	<input checked="" type="checkbox"/>				<input checked="" type="checkbox"/>	<input checked="" type="checkbox"/>				
	Gori (1983)	Recommend referring to the literature. This model considers: 1) soil absorbed water content, 2) soil permanent wilting point, 3) soil field capacity.	Uncertainties exist in parameters used in this model.										<input checked="" type="checkbox"/>		

Model category	Author	Expression	Comments	Factors involved in each model										
				λ , thermal conductivity, W/(m·K)			ϕ , volume fraction			n , porosity			S , saturation degree	
				ρ , dry density, kg/m ³			w , gravimetric moisture			T , temperature, °C			C , coefficient	
				λ_{solid}	λ_{water}	λ_{air}	ϕ_{solid}	ϕ_{water}	ϕ_{air}	n	S	ρ	w	T
	Tong et al. (2009)	$\lambda_{eff} = \frac{\eta_1(1-n)\lambda_{solid} + (1-\eta_2)[1-\eta_1(1-n)]^2}{\frac{(1-n)(1-\eta_1)}{\lambda_{solid}} + \frac{nS}{\lambda_{water}}} + \eta_2[(1-n)(1-\eta_1)\lambda_{solid}]$	Coefficients η_1 , η_2 relates to pore structure, saturation degree and temperature, which are difficult to be determined.	<input checked="" type="checkbox"/>	<input checked="" type="checkbox"/>	<input checked="" type="checkbox"/>				<input checked="" type="checkbox"/>	<input checked="" type="checkbox"/>		<input checked="" type="checkbox"/>	<input checked="" type="checkbox"/>
	Haigh (2012)	<p>Recommend referring to the literature.</p> <ol style="list-style-type: none"> 1) Based on 2D soil contact cell unit, 2) Water film formation is considered, 3) Applicable for $n > 0.33$. 	Involved coefficients are related to the thickness of water film, S and the width of water film, resulting in inconvenient implementation.	<input checked="" type="checkbox"/>	<input checked="" type="checkbox"/>	<input checked="" type="checkbox"/>					<input checked="" type="checkbox"/>			<input checked="" type="checkbox"/>
Empirical models	Kersten (1949)	$\lambda_{eff} = 0.144[0.9 \log w - 0.2]10^{1.6\rho}$, for silts or clay $\lambda_{eff} = 0.144[0.7 \log w + 0.4] \times 10^{1.6\rho}$, for sandy soils	The applicable range of w is limited.								<input checked="" type="checkbox"/>	<input checked="" type="checkbox"/>		

Model category	Author	Expression	Comments	Factors involved in each model											
				λ , thermal conductivity, W/(m·K)			ϕ , volume fraction			n , porosity			S , saturation degree		
				ρ , dry density, kg/m ³			w , gravimetric moisture			T , temperature, °C			C , coefficient		
				λ_{solid}	λ_{water}	λ_{air}	ϕ_{solid}	ϕ_{water}	ϕ_{air}	n	S	ρ	w	T	C
	Johansen (1977)	$\lambda_{eff} = \lambda_r(\lambda_{sat} - \lambda_{dry}) + \lambda_{dry}$ λ_r is the normalized thermal conductivity λ_{sat} is the saturated thermal conductivity λ_{dry} is the dry thermal conductivity	1) Proposing the concept of λ_r , 2) Obtaining λ_r by $\lambda_r \sim S$ correlation, 3) Obtaining λ_{dry} , λ_{dry} by his theoretical model.	<input checked="" type="checkbox"/>	<input checked="" type="checkbox"/>					<input checked="" type="checkbox"/>	<input checked="" type="checkbox"/>	<input checked="" type="checkbox"/>			
	Donazzi et al. (1979)	$\lambda_{eff} = \lambda_{water}^n \lambda_{solid}^{1-n} \exp[-3.08n(1-S)^2]$	Easy to implement with no coefficients.	<input checked="" type="checkbox"/>	<input checked="" type="checkbox"/>					<input checked="" type="checkbox"/>	<input checked="" type="checkbox"/>				
	Rao and Singh (1999)	$\lambda_{eff} = 10^{1.6\rho} (1.07 \log w + a)$ a is the coefficient	The coefficient is related to soils type. And $w \geq 10\%$ for clay and silts $w \geq 1\%$ for sands.									<input checked="" type="checkbox"/>	<input checked="" type="checkbox"/>		<input checked="" type="checkbox"/>
	Balland and Arp (2005)	Recommend referring to the literature.	Predicting λ_{eff} through a proposed $\lambda_r \sim S$ relationship.	<input checked="" type="checkbox"/>		<input checked="" type="checkbox"/>					<input checked="" type="checkbox"/>	<input checked="" type="checkbox"/>			<input checked="" type="checkbox"/>

Model category	Author	Expression	Comments	Factors involved in each model											
				λ , thermal conductivity, W/(m·K)			ϕ , volume fraction			n , porosity			S , saturation degree		
				ρ , dry density, kg/m ³			w , gravimetric moisture			T , temperature, °C			C , coefficient		
				λ_{solid}	λ_{water}	λ_{air}	ϕ_{solid}	ϕ_{water}	ϕ_{air}	n	S	ρ	w	T	C
	Côté and Konrad (2005)	$\lambda_{eff} = \frac{\lambda_{water}^n \lambda_{solid}^{1-n} - a 10^{-bn}}{\left[\frac{cS}{1+(c-1)S} \right] + a} + a$ 10^{-bn} $\lambda_r = \frac{cS}{1+(c-1)S}$ a, b, c are empirical coefficients	Developing $\lambda_r \sim S$ correlation as	<input checked="" type="checkbox"/>	<input checked="" type="checkbox"/>					<input checked="" type="checkbox"/>	<input checked="" type="checkbox"/>				<input checked="" type="checkbox"/>
	Lu et al. (2007)	$\lambda_{eff} = \left[\lambda_{water}^n \lambda_{solid}^{1-n} - (b - an) \times \exp [c(1 - S^{c-1.33})] + (b - an) \right]$ a, b, c are coefficients	The coefficients are related to the dry soil thermal conductivity and soil type.	<input checked="" type="checkbox"/>	<input checked="" type="checkbox"/>					<input checked="" type="checkbox"/>	<input checked="" type="checkbox"/>				<input checked="" type="checkbox"/>
	Chen (2008)	$\lambda_{eff} = \lambda_{water}^n \lambda_{solid}^{1-n} [(1 - a)S + a]^{bn}$ a, b are coefficients	This model has high accuracy for high quartz content soil. The coefficients are related to soil type.	<input checked="" type="checkbox"/>	<input checked="" type="checkbox"/>					<input checked="" type="checkbox"/>	<input checked="" type="checkbox"/>				<input checked="" type="checkbox"/>
Machine learning models	Rizvi et al. (2020a)	ANN algorithm	Only for unsaturated soil.				<input checked="" type="checkbox"/>			<input checked="" type="checkbox"/>	<input checked="" type="checkbox"/>				
	Zhang et al. (2020)	ANN algorithm	Performances using different inputs are compared.				<input checked="" type="checkbox"/>			<input checked="" type="checkbox"/>	<input checked="" type="checkbox"/>	<input checked="" type="checkbox"/>			

Model category	Author	Expression	Comments	Factors involved in each model												
				λ , thermal conductivity, W/(m·K)			ϕ , volume fraction			n , porosity			S , saturation degree			
				ρ , dry density, kg/m ³			w , gravimetric moisture			T , temperature, °C			C , coefficient			
				λ_{solid}	λ_{water}	λ_{air}	ϕ_{solid}	ϕ_{water}	ϕ_{air}	n	S	ρ	w	T	C	
	Fei et al. (2021)	ANN algorithm	Mesoscale and microscale structure factors are considered.	<input checked="" type="checkbox"/>							<input checked="" type="checkbox"/>					
	Li et al. (2022b)	Six algorithms performance are compared	Adaptive boosting methods are recommended	<input checked="" type="checkbox"/>			<input checked="" type="checkbox"/>	<input checked="" type="checkbox"/>			<input checked="" type="checkbox"/>	<input checked="" type="checkbox"/>		<input checked="" type="checkbox"/>	<input checked="" type="checkbox"/>	
	Zhao et al. (2022)	Seven algorithms performance are compared	Neural networks are recommended				<input checked="" type="checkbox"/>				<input checked="" type="checkbox"/>		<input checked="" type="checkbox"/>	<input checked="" type="checkbox"/>		

476 4 Research gaps and a methodological framework for futures studies

477 Based on the review regarding the factors influencing soil λ_{eff} and the models for the λ_{eff} prediction,
478 a holistic view of research gaps is given, followed by detailed explanations. Then, a methodological
479 framework for future studies is proposed.

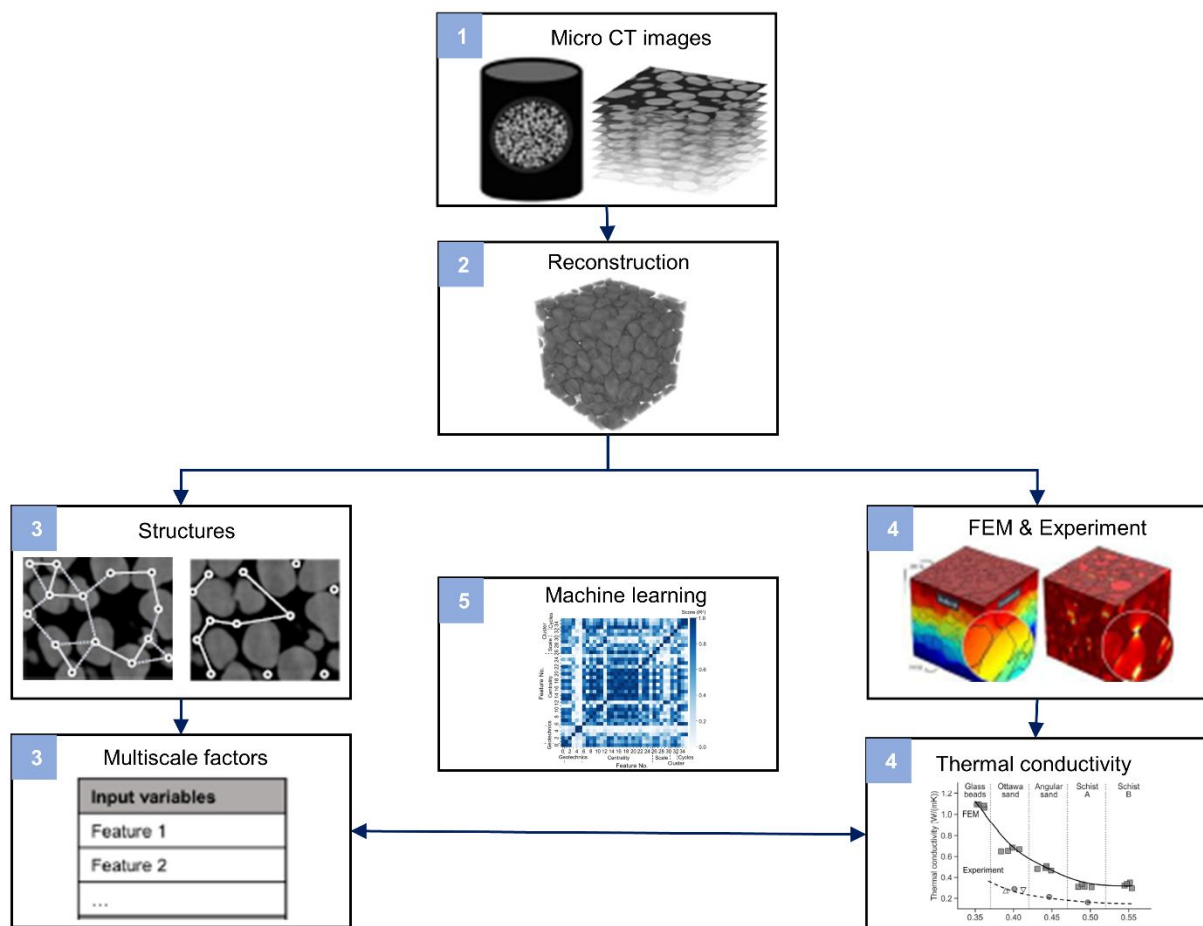
480 In addition to the intrinsic properties of soil, its structure is an underlying factor that influences thermal
481 conductivity, as it determines the structure of heat transfer pathways. Other factors, such as water
482 content and gradation, also affect thermal conductivity by creating new structures for heat transfer
483 pathways. Previous research has investigated the impact of soil structure on thermal conductivity in dry
484 conditions; however, in unsaturated conditions, the addition of water connects soil particles, resulting
485 in a different soil structure. Lu and McCartney (2024) and Lu and Dong (2015) have linked the different
486 mechanisms of water retention to thermal conductivity. However, the altered heat transfer pathways
487 due to the addition of water, which are underlying reasons contributing to an increase in thermal
488 conductivity, remain an unexplored area of research. Furthermore, existing research on soil thermal
489 conductivity has effectively utilised complex network theory to quantify soil structure, establishing
490 correlations between network-derived features and thermal conductivity in dry conditions. This
491 innovative approach marks a significant advancement in understanding soil behaviour. However,
492 complex network theory alone may not fully capture the soil structure under unsaturated conditions
493 where the structure undergoes notable changes due to water addition. In this light, the potential of other
494 structural quantification methods should be explored. The alternative methods discussed below offer
495 diverse perspectives on soil structure quantification, yet their parameters have not been investigated in
496 relation to soil thermal conductivity.

497 Euler number is a topological invariant, and it is expressed as (Herring 2012; Herring et al. 2013;
498 Herring et al. 2019)

$$\chi = \beta_0 - \beta_1 + \beta_2 \quad (8)$$

499 where χ is the Euler number; β_0 is the zeroth Betti number, representing the number of discrete elements
500 in the volume; β_1 is the first Betti number, indicating the number of redundant loops in the structure;
501 and β_2 is the second Betti number, referring to the number of cavities. Herring et al. (2013) used it to
502 quantify the connectivity of nonwetting phase in porous media. However, the connectivity of soil pores
503 that are based on Euler number has not been studied from the perspective of λ_{eff} . In addition, statistical
504 approaches are also favourable to the description of soil structures. Minkowski functions are geometric
505 measurements that can quantify the soil structure statistically based on computed tomography images
506 of soil (Vogel et al. 2010). Specifically, the zeroth Minkowski function indicates total mass of the
507 studied object (pore or solid); the first Minkowski function represents the interfacial area between pore
508 and solid; the second is the interface's mean curvature; the third measures the total curvature (Vogel et
509 al. 2010). The underlying theorem for using Minkowski functions to quantify the soil structure is
510 proposed by Hadwiger (2013); he claimed that any properties, related only to the object's form, can be
511 expressed by a combination of Minkowski functions. However, the relationship between Minkowski
512 functions and soil λ_{eff} has not been researched. Furthermore, the particle or pore connectivity does not
513 consider the local geometries (e.g., shape and size) of individual particles or pores; similarly, the local
514 geometries (e.g., shape and size) do not include global information (e.g., particle or pore connectivity).
515 But the soil λ_{eff} depends on both the global and local geometries. Persistent homology analysis can
516 measure the global and local characteristic simultaneously (Herring et al. 2019). Therefore, parameters
517 derived from persistent homology analysis could contribute to the comprehensive understanding of soil
518 the λ_{eff} ; whereas they have not been studied from heat transfer aspect. A parameter describing the
519 extent of the transition from disorder to order in a granular system is proposed by Dai et al. (2019),
520 which could also be introduced to soil structures quantification.

521 As previously pointed out, it is essential to quantify soil structure not only in dry conditions but also
 522 under unsaturated conditions to better understand the relationship between structural quantification and
 523 thermal conductivity. The goal of this endeavour is to include structural quantifications for thermal
 524 conductivity prediction. However, it is crucial to recognise that soil thermal conductivity is also
 525 influenced by other factors at various scales in addition to structural quantifications (Table 1). Therefore,
 526 a comprehensive framework that considers those additional factors presented in Table 1 is necessary
 527 for accurate prediction of thermal conductivity. Current models for predicting soil thermal conductivity
 528 fall short in this regard, as they do not fully account for all influencing factors, particularly the varied
 529 structure of unsaturated soils. The application of machine learning presents a promising avenue for
 530 developing a more integrative model (Fei et al. 2021). Current machine learning-based models in this
 531 field, however, have not yet fully incorporated soil structure data from both dry and unsaturated
 532 conditions as inputs. This limitation underscores the need for an updated machine learning framework
 533 that is designed to process and learn from a comprehensive set of inputs. By integrating detailed
 534 structural data from varying soil conditions along with other relevant factors at different scales, a
 535 framework is proposed in Figure 9, which could advance our capability to predict soil thermal
 536 conductivity with higher accuracy and relevance to real-world scenarios.



537

538 *Figure 9 Framework of investigation on unsaturated soil effective thermal conductivity through multiscale*
 539 *characters; tools for each stage could be: 1) computed tomography imaging equipment; 2) software including*
 540 *ImageJ, Simpleware ScanIP; 3) network approaches or statistical methods; 4) finite element modelling and*
 541 *experimental measurements and 5) Python.*

542 Firstly, modern computed tomography devices are employed to scan real soil samples (dry/unsaturated)
 543 and produce high resolution 3D image stacks. Afterwards, these images are used to reconstruct the 3D
 544 samples digitally by image process tools. The reconstructed 3D models serve as the foundation for both
 545 structural quantification and heat transfer processes modelling. The structural quantification relies on

546 network approaches or statistical methods. Meanwhile, Finite Element Modelling (FEM) is adopted to
547 simulate heat transfer processes to compute λ_{eff} , which will be further validated by measurements.
548 Machine learning techniques are employed to discern the relationship between thermal conductivity
549 and a combination of structural parameters and other traditional factors at multiple scales, including but
550 not limited to solid particle thermal conductivity, porosity, and degree of saturation.

551 5 Conclusion

552 In this review, we systematically examined the various factors influencing soil thermal conductivity.
553 Our findings highlight that soil structure impacts thermal conductivity significantly, but this area of
554 research remains relatively unexplored due to the lack of characterising particle connectivity. A
555 relationship between thermal conductivity and soil structure has been previously studied under dry
556 conditions through the application of complex network theory for structural quantification. However,
557 soil structure that undergoes notable changes due to the addition of water under unsaturated conditions
558 has not been well characterised. Given the increased complexity of soil structure in unsaturated
559 conditions compared to dry conditions, relying solely on complex network theory might be insufficient
560 to capture the complete structural information. Consequently, we have explored other potential methods
561 for a more comprehensive quantification of soil structure.

562 Furthermore, it is crucial to recognize that soil thermal conductivity is influenced not just by structural
563 factors but also by a range of other variables. Our investigation reveals that current models for predicting
564 soil thermal conductivity fall short of incorporating the full spectrum of influencing factors. To bridge
565 this gap, we proposed a new integrative framework that considers both structural parameters and other
566 relevant factors across different scales. This framework employs soil computed tomography (CT)
567 images. These images offer a robust physical basis for an accurate description of soil structures based
568 on quantification methods. Moreover, the framework integrates machine learning approaches,
569 capitalising on their ability to assimilate a multitude of factors as inputs when predicting effective
570 thermal conductivity. Machine learning's inherent strength in pattern recognition and data integration
571 makes it particularly suited for this task. By combining the detailed structural data with other relevant
572 factors, our framework aims to enhance the accuracy and applicability of predictive models, offering a
573 more holistic understanding of soil thermal conductivity.

574 CrediT authorship contribution statement

575 **Tairu Chen:** Conceptualization, Data curation, Methodology, Formal analysis, Writing – original draft;
576 Writing – review & editing., **Wenbin Fei:** Methodology, Writing – review & editing, Supervision.,
577 **Guillermo A. Narsilio:** Writing – review & editing, Supervision, Project administration, Funding
578 acquisition.

579 Declaration of Competing Interest

580 The authors declare that they have no known competing financial interests or personal relationships that
581 could have appeared to influence the work reported in this paper.

582 Acknowledgements

583 The authors acknowledge the funding provided by the Australian Research Council project
584 DP210100433 and China Scholarship Council (CSC)-University of Melbourne Scholarship provided
585 by the CSC and The University of Melbourne.

586 Data Availability

587 Data generated or analysed during this study are available from the corresponding author upon
588 reasonable request.

References

- Abu-Hamdeh, N.H. 2003. Thermal properties of soils as affected by density and water content. *Biosystems Engineering*, **86**(1):97-102.
- Agrawal, K.K., Yadav, T., Misra, R., and Agrawal, G.D. 2019. Effect of soil moisture contents on thermal performance of earth-air-pipe heat exchanger for winter heating in arid climate: In situ measurement. *Geothermics*, **77**:12-23.
- Asakuma, Y., Kanazawa, Y., and Yamamoto, T. 2014. Thermal radiation analysis of packed bed by a homogenization method. *International Journal of Heat and Mass Transfer*, **73**:97-102.
- Balland, V., and Arp, P.A. 2005. Modeling soil thermal conductivities over a wide range of conditions. *Journal of Environmental Engineering and Science*, **4**(6):549-558.
- Bauer, S., Beyer, C., Dethlefsen, F., Dietrich, P., Duttmann, R., Ebert, M., Feeser, V., Görke, U., Köber, R., and Kolditz, O. 2013. Impacts of the use of the geological subsurface for energy storage: an investigation concept. *Environmental earth sciences*, **70**(8):3935-3943.
- Birch, A.F., and Clark, H. 1940. The thermal conductivity of rocks and its dependence upon temperature and composition. *American Journal of Science*, **238**(8):529-558.
- Brandl, H. 2006. Energy foundations and other thermo-active ground structures. *Géotechnique*, **56**(2):81-122.
- Campbell, G., Jungbauer Jr, J., Bidlake, W., and Hungerford, R. 1994. Predicting the effect of temperature on soil thermal conductivity. *Soil science*, **158**(5):307-313.
- Carter, M.R., and Gregorich, E.G. (2007) *Soil sampling and methods of analysis*. CRC press.
- Chen, S.X. 2008. Thermal conductivity of sands. *Heat and mass transfer*, **44**(10):1241-1246.
- Cheng, G., Yu, A., and Zulli, P. 1999. Evaluation of effective thermal conductivity from the structure of a packed bed. *Chemical Engineering Science*, **54**(19):4199-4209.
- Cherkasova, A.S., and Shan, J.W. 2008. Particle aspect-ratio effects on the thermal conductivity of micro-and nanoparticle suspensions. *Journal of Heat Transfer*, **130**(8).
- Côté, J., and Konrad, J.-M. 2005. A generalized thermal conductivity model for soils and construction materials. *Canadian Geotechnical Journal*, **42**(2):443-458.

- Cox, M.R., and Budhu, M. 2008. A practical approach to grain shape quantification. *Engineering Geology*, **96**(1-2):1-16.
- Cui, S.-Q., Zhou, C., Liu, J.-Q., and Akinniyi, D.B. 2023. Stress effects on thermal conductivity of soils and heat transfer efficiency of energy piles in the saturated and unsaturated soils. *Computers and Geotechnics*, **160**:105549.
- Dai, W., Hanaor, D., and Gan, Y. 2019. The effects of packing structure on the effective thermal conductivity of granular media: A grain scale investigation. *International Journal of Thermal Sciences*, **142**:266-279.
- De Vries, D., and Van Wijk, W. 1963. Physics of plant environment. *Environmental control of plant growth*, **5**:69.
- De Vries, D.A. 1963. Thermal properties of soils. *Physics of plant environment*.
- Ding, H., Han, Z., Li, Y., Xie, W., Fu, B., Li, C., and Zhao, L. 2023. Particle breakage and its mechanical response in granular soils: A review and prospect. *Construction and Building Materials*, **409**:133948.
- Donazzi, F., Occhini, E., and Seppi, A. 1979. Soil thermal and hydrological characteristics in designing underground cables. In *Proceedings of the Institution of Electrical Engineers*. IET, vol. 126, pp. 506-516.
- Dong, Y., McCartney, J.S., and Lu, N. 2015. Critical Review of Thermal Conductivity Models for Unsaturated Soils. *Geotechnical and Geological Engineering*, **33**(2):207-221.
- El Shamy, U., De Leon, O., and Wells, R. 2013. Discrete element method study on effect of shear-induced anisotropy on thermal conductivity of granular soils. *International Journal of Geomechanics*, **13**(1):57-64.
- Fei, W., and Narsilio, G.A. 2020. Network analysis of heat transfer in sands. *Computers and Geotechnics*, **127**:103773.
- Fei, W., Narsilio, G.A., and Disfani, M.M. 2019a. Impact of three-dimensional sphericity and roundness on heat transfer in granular materials. *Powder Technology*, **355**:770-781.

- Fei, W., Narsilio, G.A., and Disfani, M.M. 2021. Predicting effective thermal conductivity in sands using an artificial neural network with multiscale microstructural parameters. *International Journal of Heat and Mass Transfer*, **170**:120997.
- Fei, W., Narsilio, G.A., Van Der Linden, J.H., and Disfani, M.M. 2019b. Quantifying the impact of rigid interparticle structures on heat transfer in granular materials using networks. *International Journal of Heat and Mass Transfer*, **143**:118514.
- Fei, W., Narsilio, G.A., Van Der Linden, J.H., and Disfani, M.M. 2020. Network analysis of heat transfer in sphere packings. *Powder Technology*, **362**:790-804.
- Fei, W.B., Li, Q., Wei, X.C., Song, R.R., Jing, M., and Li, X.C. 2015. Interaction analysis for CO₂ geological storage and underground coal mining in Ordos Basin, China. *Engineering Geology*, **196**:194-209.
- Feng, Y., Han, K., and Owen, D. 2009. Discrete thermal element modelling of heat conduction in particle systems: pipe-network model and transient analysis. *Powder Technology*, **193**(3):248-256.
- Finney, J. 1970. Random packings and the structure of simple liquids. I. The geometry of random close packing. *Proceedings of the Royal Society of London. A. Mathematical and Physical Sciences*, **319**(1539):479-493.
- Gan, J., Zhou, Z., and Yu, A. 2017. Effect of particle shape and size on effective thermal conductivity of packed beds. *Powder Technology*, **311**:157-166.
- Gori, F. 1983. A theoretical model for predicting the effective thermal conductivity of unsaturated frozen soils. In *Proceedings of the fourth international conference on Permafrost, Fairbanks (Alaska)*. National Academy Press Washington, DC, vol. 363.
- Gori, F., and Corasaniti, S. 2002. Theoretical prediction of the soil thermal conductivity at moderately high temperatures. *J. Heat Transfer*, **124**(6):1001-1008.
- Grabarczyk, M., and Furmański, P. 2013. Predicting the effective thermal conductivity of dry granular media using artificial neural networks. *Journal of Power Technologies*, **93**(2):59-66.
- Hadwiger, H. (2013) *Vorlesungen über Inhalt, Oberfläche und isoperimetrie*. Springer-Verlag.
- Haigh, S. 2012. Thermal conductivity of sands. *Géotechnique*, **62**(7):617-625.

- Hamilton, R.L., and Crosser, O. 1962. Thermal conductivity of heterogeneous two-component systems. *Industrial & Engineering chemistry fundamentals*, **1**(3):187-191.
- Hashin, Z., and Shtrikman, S. 1962. A variational approach to the theory of the effective magnetic permeability of multiphase materials. *Journal of applied Physics*, **33**(10):3125-3131.
- He, H., Li, M., Dyck, M., Si, B., Wang, J., and Lv, J. 2020. Modelling of soil solid thermal conductivity. *International Communications in Heat and Mass Transfer*, **116**:104602.
- Herring, A., Robins, V., and Sheppard, A. 2019. Topological persistence for relating microstructure and capillary fluid trapping in sandstones. *Water Resources Research*, **55**(1):555-573.
- Herring, A.L. 2012. Saturation, morphology, and topology of nonwetting phase fluid in bentheimer sandstone; application to geologic sequestration of supercritical CO₂.
- Herring, A.L., Harper, E.J., Andersson, L., Sheppard, A., Bay, B.K., and Wildenschild, D. 2013. Effect of fluid topology on residual nonwetting phase trapping: Implications for geologic CO₂ sequestration. *Advances in water resources*, **62**:47-58.
- Hiraiwa, Y., and Kasubuchi, T. 2000. Temperature dependence of thermal conductivity of soil over a wide range of temperature (5–75 C). *European Journal of Soil Science*, **51**(2):211-218.
- Hryciw, R.D., Zheng, J., and Shetler, K. 2016. Particle roundness and sphericity from images of assemblies by chart estimates and computer methods. *Journal of Geotechnical and Geoenvironmental Engineering*, **142**(9):04016038.
- Jia, G., Tao, Z., Meng, X., Ma, C., Chai, J., and Jin, L. 2019. Review of effective thermal conductivity models of rock-soil for geothermal energy applications. *Geothermics*, **77**:1-11.
- Jin, H., Wang, Y., Zheng, Q., Liu, H., and Chadwick, E. 2017. Experimental Study and Modelling of the Thermal Conductivity of Sandy Soils of Different Porosities and Water Contents. *Applied Sciences-Basel*, **7**(2).
- Johansen, O. (1977) *Thermal conductivity of soils*.
- Kayaci, N., and Demir, H. 2018. Numerical modelling of transient soil temperature distribution for horizontal ground heat exchanger of ground source heat pump. *Geothermics*, **73**:33-47.
- Kersten, M.S. 1949. Laboratory research for the determination of thermal properties of soils.

- Lee, C., Suh, H.S., Yoon, B., and Yun, T.S. 2017. Particle shape effect on thermal conductivity and shear wave velocity in sands. *Acta Geotechnica*, **12**(3):615-625.
- Lees, G. 1964. A new method for determining the angularity of particles. *Sedimentology*, **3**(1):2-21.
- Li, K.-Q., Kang, Q., Nie, J.-Y., and Huang, X.-W. 2022a. Artificial neural network for predicting the thermal conductivity of soils based on a systematic database. *Geothermics*, **103**:102416.
- Li, K.-Q., Liu, Y., and Kang, Q. 2022b. Estimating the thermal conductivity of soils using six machine learning algorithms. *International Communications in Heat and Mass Transfer*, **136**:106139.
- Liu, C., Zhou, D., and Wu, H. 2011. Measurement and prediction of temperature effects of thermal conductivity of soils. *Chinese Journal of Geotechnical Engineering*, **33**(12):1877-1886.
- Lu, N., and Dong, Y. 2015. Closed-form equation for thermal conductivity of unsaturated soils at room temperature. *Journal of Geotechnical and Geoenvironmental Engineering*, **141**(6):04015016.
- Lu, S., and Ren, T. 2009. Model for predicting soil thermal conductivity at various temperatures. *Transactions of the Chinese Society of Agricultural Engineering*, **25**(7):13-18.
- Lu, S., Ren, T., Gong, Y., and Horton, R. 2007. An improved model for predicting soil thermal conductivity from water content at room temperature. *Soil Science Society of America Journal*, **71**(1):8-14.
- Lu, Y., and McCartney, J.S. 2024. Thermal conductivity function for fine-grained unsaturated soils linked with water retention by capillarity and adsorption. *Journal of Geotechnical and Geoenvironmental Engineering*, **150**(1):06023009.
- Midttomme, K., and Roaldset, E. 1998. The effect of grain size on thermal conductivity of quartz sands and silts. *Petroleum Geoscience*, **4**(2):165-172.
- Mirmohammadi, S.A., Behi, M., Gan, Y., and Shen, L. 2019. Particle-shape-, temperature-, and concentration-dependent thermal conductivity and viscosity of nanofluids. *Physical Review E*, **99**(4):043109.
- Morimoto, T., O'sullivan, C., and Taborda, D.M. 2022. Exploiting DEM to Link Thermal Conduction and Elastic Stiffness in Granular Materials. *Journal of Engineering Mechanics*, **148**(2):04021139.

- Narsilio, G.A., Kress, J., and Yun, T.S. 2010. Characterisation of conduction phenomena in soils at the particle-scale: Finite element analyses in conjunction with synthetic 3D imaging. *Computers and Geotechnics*, **37**(7-8):828-836.
- Newman, M.E. 2003. The structure and function of complex networks. *SIAM review*, **45**(2):167-256.
- Peeketi, A.R., Moscardini, M., Papeschi, S., Gan, Y., Kamlah, M., and Annabattula, R.K. 2019. Analytical estimation of the effective thermal conductivity of a granular bed in a stagnant gas including the Smoluchowski effect. *Granular matter*, **21**:1-21.
- Rao, M.G., and Singh, D.N. 1999. A generalized relationship to estimate thermal resistivity of soils. *Canadian Geotechnical Journal*, **36**(4):767-773.
- Rizvi, Z.H., Akhtar, S.J., Sabeeh, W.T., and Wuttke, F. 2020a. Effective thermal conductivity of unsaturated soils based on deep learning algorithm. In *E3S Web of Conferences*. EDP Sciences, vol. 205, pp. 04006.
- Rizvi, Z.H., Husain, S.M.B., Haider, H., and Wuttke, F. 2020b. Effective thermal conductivity of sands estimated by Group Method of Data Handling (GMDH). *Materials Today: Proceedings*, **26**:2103-2107.
- Rizvi, Z.H., Zaidi, H.H., Akhtar, S.J., Sattari, A.S., and Wuttke, F. 2020c. Soft and hard computation methods for estimation of the effective thermal conductivity of sands. *Heat and mass transfer*: 1-13.
- Schimmel, M., Liu, W., and Worrell, E. 2019. Facilitating sustainable geo-resources exploitation: A review of environmental and geological risks of fluid injection into hydrocarbon reservoirs. *Earth-Science Reviews*, **194**:455-471.
- Sepaskhah, A., and Boersma, L. 1979. Thermal conductivity of soils as a function of temperature and water content. *Soil Science Society of America Journal*, **43**(3):439-444.
- Slusarchuk, W.A., and Watson, G.H. 1975. Thermal conductivity of some ice-rich permafrost soils. *Canadian Geotechnical Journal*, **12**(3):413-424.
- Smits, K.M., Sakaki, T., Howington, S.E., Peters, J.F., and Illangasekare, T.H. 2013. Temperature dependence of thermal properties of sands across a wide range of temperatures (30–70 C). *Vadose Zone Journal*, **12**(1):vzj2012.0033.

- Tarnawski, V., Momose, T., and Leong, W. 2009. Assessing the impact of quartz content on the prediction of soil thermal conductivity. *Géotechnique*, **59**(4):331-338.
- Tong, F., Jing, L., and Zimmerman, R.W. 2009. An effective thermal conductivity model of geological porous media for coupled thermo-hydro-mechanical systems with multiphase flow. *International Journal of Rock Mechanics and Mining Sciences*, **46**(8):1358-1369.
- Vaferi, B., Gitifar, V., Darvishi, P., and Mowla, D. 2014. Modeling and analysis of effective thermal conductivity of sandstone at high pressure and temperature using optimal artificial neural networks. *Journal of petroleum science and engineering*, **119**:69-78.
- Vargas, W.L., and McCarthy, J.J. 2001. Heat conduction in granular materials. *AIChE Journal*, **47**(5):1052-1059.
- Verma, L., Shrotriya, A., Singh, R., and Chaudhary, D. 1991. Thermal conduction in two-phase materials with spherical and non-spherical inclusions. *Journal of Physics D: Applied Physics*, **24**(10):1729.
- Vogel, H.-J., Weller, U., and Schlüter, S. 2010. Quantification of soil structure based on Minkowski functions. *Computers & Geosciences*, **36**(10):1236-1245.
- Wadell, H. 1932. Volume, shape, and roundness of rock particles. *The Journal of Geology*, **40**(5):443-451.
- Wei, H., Zhao, S., Rong, Q., and Bao, H. 2018. Predicting the effective thermal conductivities of composite materials and porous media by machine learning methods. *International Journal of Heat and Mass Transfer*, **127**:908-916.
- Weidenfeld, G., Weiss, Y., and Kalman, H. 2004. A theoretical model for effective thermal conductivity (ETC) of particulate beds under compression. *Granular matter*, **6**(2-3):121-129.
- Wiener, O. 1912. *Abhandl. math.-phys. Kl. Königl. Sachsischen Gesell.*, **32**:509.
- Xiao, Y., Liu, H., Nan, B., and McCartney, J.S. 2018. Gradation-dependent thermal conductivity of sands. *Journal of Geotechnical and Geoenvironmental Engineering*, **144**(9):06018010.
- Xiao, Y., Ma, G., Nan, B., and McCartney, J.S. 2020. Thermal conductivity of granular soil mixtures with contrasting particle shapes. *Journal of Geotechnical and Geoenvironmental Engineering*, **146**(5):06020004.

- Yun, T.S., and Evans, T.M. 2010. Three-dimensional random network model for thermal conductivity in particulate materials. *Computers and Geotechnics*, **37**(7-8):991-998.
- Yun, T.S., and Santamarina, J.C. 2008. Fundamental study of thermal conduction in dry soils. *Granular matter*, **10**(3):197-207.
- Zhang, N., and Wang, Z.Y. 2017. Review of soil thermal conductivity and predictive models. *International Journal of Thermal Sciences*, **117**:172-183.
- Zhang, N., Yu, X., Pradhan, A., and Puppala, A.J. 2015a. Effects of particle size and fines content on thermal conductivity of quartz sands. *Transportation Research Record*, **2510**(1):36-43.
- Zhang, N., Yu, X., Pradhan, A., and Puppala, A.J. 2015b. Thermal conductivity of quartz sands by thermo-time domain reflectometry probe and model prediction. *Journal of Materials in Civil Engineering*, **27**(12):04015059.
- Zhang, N., Zou, H., Zhang, L., Puppala, A.J., Liu, S., and Cai, G. 2020. A unified soil thermal conductivity model based on artificial neural network. *International Journal of Thermal Sciences*, **155**:106414.
- Zhang, T., Cai, G., Liu, S., and Puppala, A.J. 2017. Investigation on thermal characteristics and prediction models of soils. *International Journal of Heat and Mass Transfer*, **106**:1074-1086.
- Zhao, T., Liu, S., Xu, J., He, H., Wang, D., Horton, R., and Liu, G. 2022. Comparative analysis of seven machine learning algorithms and five empirical models to estimate soil thermal conductivity. *Agricultural and Forest Meteorology*, **323**:109080.
- Zhou, B., Wang, J., and Wang, H. 2018. Three-dimensional sphericity, roundness and fractal dimension of sand particles. *Géotechnique*, **68**(1):18-30.
- Zhou, Z., Yu, A., and Zulli, P. 2010. A new computational method for studying heat transfer in fluid bed reactors. *Powder Technology*, **197**(1-2):102-110.

List of Figures

Figure 1 Influence of solid particle thermal conductivity $\lambda_{particle}$ on soil effective thermal conductivity λ_{eff} under different porosity based on data from He et al. (2020)

Figure 2 The distribution of soil effective thermal conductivity λ_{eff} with porosity: (a) dry soils with data from Slusarchuk and Watson (1975); Johansen (1977); Côté and Konrad (2005); Yun and Santamarina (2008); Narsilio et al. (2010); Fei et al. (2019b); χ and η are 0.75 W/(m·K) and 1.2 for generating Eq. (3); $\lambda_{particle}$, λ_{air} and S are 2 W/(m·K), 0.026 W/(m·K) and 0 for generating Eq. (1); (b) unsaturated / saturated soils predicted values using Eq. (1) with $\lambda_{particle}=5$ W/(m·K), $\lambda_{water}=0.56$ W/(m·K), $\lambda_{air}=0.026$ W/(m·K); quartzite and granite experimental data is from Côté and Konrad (2005)

Figure 3 Network features illustration based on complex network theory from (Fei and Narsilio 2020)

Figure 4 Influence of contact area-weighted degree in complex network theory on soil effective thermal conductivity λ_{eff} in with data from Fei et al. (2021)

Figure 5 Influence of particle shape on soil effective thermal conductivity λ_{eff} (a) shape defined by surface areas with dry glass experimental data from Verma et al. (1991); λ_{solid} is around 1 W/(m·K), λ_{air} is around 0.025 W/(m·K); (b) shape defined by Eq. (5) and Eq. (6) with data from Fei et al. (2019a); $\lambda_{solid} = 3$ W/(m·K), $\lambda_{air} = 0.025$ W/(m·K), $\lambda_{water} = 0.591$ W/(m·K)

Figure 6 Influence of particle size on soil effective thermal conductivity λ_{eff} with data from Midttomme and Roaldset (1998); Chen (2008); Lee et al. (2017); Fei et al. (2021)

Figure 7 Influence of degree of saturation on soil effective thermal conductivity λ_{eff} with data from De Vries (1963); Johansen (1977); Côté and Konrad (2005); Lu et al. (2007); Chen (2008); Zhang et al. (2015b)

Figure 8 Influence of temperature on soil effective thermal conductivity λ_{eff} with experimental data selected from (a) quincy sand at different volumetric water content (Campbell et al. 1994) and (b) clay loam at different volumetric water content (Hiraiwa and Kasubuchi 2000)

Figure 9 Framework of investigation on unsaturated soil effective thermal conductivity through multiscale characters; tools for each stage could be: 1) computed tomography imaging equipment; 2) software including ImageJ, Simpleware ScanIP; 3) network approaches or statistical methods; 4) finite element modelling and experimental measurements and 5) Python.

List of Tables

Table 1 Categories of the factors influencing soil effective thermal conductivity

Table 2 Indices of soil particle connectivity at mesoscale based complex network theory and their relationship with soil effective thermal conductivity λ_{eff} (Fei and Narsilio 2020; Fei et al. 2020)

Table 3 Summary of prediction models for soil effective thermal conductivity λ_{eff}